1   **Chemical Composition and Hydrolysis of Organic Nitrate Aerosol Formed from Hydroxyl and**

2   **Nitrate Radical Oxidation of α-pinene and β-pinene**

4   Masayuki Takeuchi[1] and Nga L. Ng[2,3*]

5   [1]School of Civil and Environmental Engineering, Georgia Institute of Technology, Atlanta, Georgia, 30332,

6   USA

7   [2]School of Chemical and Bimolecular Engineering, Georgia Institute of Technology, Atlanta, Georgia,

8   30332, USA

9   [3]School of Earth and Atmospheric Sciences, Georgia Institute of Technology, Atlanta, Georgia, 30332,

10   USA

11   [*]Corresponding author: ng@chbe.gatech.edu

13   **Keywords**

14   Aerosol, chemical composition, hydrolysis, monoterpenes, organic nitrate, hydroxyl and nitrate radical

15   oxidation

17 **Abstract**

18   Atmospheric organic nitrate (ON) is thought to play a crucial role in the formation potential of

19 ozone and aerosol, which are the leading air pollutants of concern across the world. Limited fundamental

20 knowledge and understanding of the life cycles of ON currently hinders the ability to quantitatively assess

21 its impacts on the formation of these pollutants. Although hydrolysis is currently considered as an important

22 loss mechanism of ON based on prior field measurement studies, this process for atmospherically relevant

23 ON has not been well constrained by fundamental laboratory studies. In this comprehensive study, we

24 investigated the chemical composition and hydrolysis process of particulate ON ($_p$ON) formed from the

25 oxidation of α-pinene and β-pinene by hydroxyl and nitrate radicals. For $_p$ON that undergoes hydrolysis,

26 the hydrolysis lifetime is determined to be no more than 30 min for all systems explored. This is

27 significantly shorter than those reported in previous chamber studies (i.e., 3-6 h) but is consistent with the

28 reported lifetime from bulk solution measurement studies (i.e., 0.02-8.8 h). The discrepancy appears to stem

29 from the choice of proxy used to estimate the hydrolysis lifetime. The measured hydrolyzable fractions of

30 $_p$ON (F_H) in the α-pinene+OH, β-pinene+OH, α-pinene+NO$_3$, and β-pinene+NO$_3$ systems are 23-32, 27-

31 34, 9-17, and 9-15 %, respectively. While a very low F_H for the nitrate radical oxidation system is expected

32 based on prior studies, F_H for the hydroxyl radical oxidation system is surprisingly lower than predicted in

33 past studies. Overall, the hydrolysis lifetime as well as F_H obtained in this study serve as experimentally

34 constrained parameters that are required in regional and global chemical transport models to accurately

35 evaluate the impacts of ON on nitrogen budget and formation of ozone and aerosol.

1. Introduction

The oxidation of biogenic volatile organic compounds (BVOC) by ozone (O_3), hydroxyl radicals and nitrate radicals is a major source of secondary organic aerosol (SOA) globally (Kanakidou et al., 2005; Goldstein and Galbally, 2007; Spracklen et al., 2011). Many studies have pointed to the synergistic effects of anthropogenic emissions on biogenic SOA formation in the atmosphere (Weber et al., 2007; Carlton et al., 2010; Hoyle et al., 2011; Shilling et al., 2013; Xu et al., 2015a; Shrivastava et al., 2019). The oxidation of BVOC in environments with anthropogenic NO_x emissions is an important mechanism for coupled biogenic-anthropogenic interactions. In the presence of NO_x, the oxidation of BVOC can lead to the formation of organic nitrate (ON), a large component of reactive oxidized nitrogen. Results from ambient field measurements have revealed the ubiquitous presence of particulate ON ($_pON$), where it contributes to a large fraction of submicron organic aerosol at different sites worldwide (Fry et al., 2013; Xu et al., 2015b; Liu et al., 2012a; Rollins et al., 2012; Rollins et al., 2013; Lee et al., 2016; Kiendler-Scharr et al., 2016; Ng et al., 2017). These findings highlights the importance to understand the formation and fates of ON to accurately evaluate its roles in NO_x recycling, O_3, and SOA formation.

Monoterpenes ($C_{10}H_{16}$) is a major class of BVOC, with annual emissions of 157-177 Tg C yr^{-1} (Guenther et al., 2012). Laboratory studies have demonstrated that the nitrate radical oxidation of monoterpenes leads to a substantial formation of ON and SOA, with ON yields up to ~70% (Wangberg et al., 1997; Berndt and Boge, 1997; Griffin et al., 1999; Hallquist et al., 1999; Spittler et al., 2006; Fry et al., 2009; Fry et al., 2014; Boyd et al., 2015; Nah et al., 2016; Boyd et al., 2017; Slade et al., 2017; Claflin and Ziemann, 2018). For photooxidation of monoterpenes in the presence of NO_x, ON yields as high as 26% have been reported for α-pinene (Noziere et al., 1999; Aschmann et al., 2002; Rindelaub et al., 2015). Monoterpene emissions do not depend strongly on light and typically continue at night, making them important ON and SOA precursors at any times of the day (daytime and nighttime) and throughout the year (different seasons). It has been shown that monoterpene-derived ON is prevalent in areas where there are substantial biogenic-anthropogenic interactions and oxidation of monoterpenes contributes to a large

62   fraction of SOA observed in the Southeastern U.S. (Xu et al., 2015a; Xu et al., 2015b; Lee et al., 2016;

63   Zhang et al., 2018; Xu et al., 2018a).

64   One of the largest uncertainties in our understanding of monoterpene ON chemistry is the extent to

65   which ON act as a permanent sink versus temporary reservoir of NO_x (Takeuchi and Ng, 2018). This would

66   depend on the fates of ON as they can either retain or release NO_x upon further reactions. Once formed,

67   gas-phase ON can undergo photolysis or hydroxyl radical oxidation to release NO_x or partition into the

68   particle phase. $_pON$ in turn can undergo further chemistry to release NO_x or hydrolyze in the particle phase

69   to form nitric acid (HNO_3). Further, ON and HNO_3 can be removed via dry and wet deposition. One

70   important reaction of ON in the particle phase is hydrolysis in the presence of aerosol water, which is a

71   mechanism for NO_x loss (Day et al., 2010; Russell et al., 2011). Studies with bulk solutions showed that

72   particle-phase hydrolysis of tertiary nitrate is fast with a lifetime of minutes, while primary and secondary

73   nitrate is stable (Darer et al., 2011; Hu et al., 2011). However, the hydrolysis of $_pON$ in aerosol water is

74   largely unconstrained. Results from field and modeling studies suggested a $_pON$ lifetime of a few hours

75   (Pye et al., 2015; Lee et al., 2016; Fisher et al., 2016; Zare et al., 2018). A few recent laboratory chamber

76   studies elicited a complex picture where $_pON$ formed from photochemical oxidation and nitrate radical

77   oxidation of monoterpenes appear to experience different magnitudes of hydrolysis (Boyd et al., 2015;

78   Rindelaub et al., 2015; Bean and Hildebrandt Ruiz, 2016; Boyd et al., 2017), likely due to the difference in

79   the relative amount of primary, secondary, and tertiary nitrate in these oxidation systems. Overall, there are

80   very limited studies on the further evolutions of ON produced from the oxidation of monoterpenes.

81   Here, we present results from a laboratory chamber study on the chemical composition and

82   hydrolysis process of $_pON$ formed from oxidation of α-pinene and β-pinene by hydroxyl and nitrate radicals.

83   Specifically, we report the hydrolysis lifetimes and the fraction of hydrolyzable $_pON$ formed in the systems

84   examined in this study. This comprehensive chamber study on the hydrolysis of $_pON$ produced from various

85   oxidation pathways of monoterpenes and peroxy radical (RO_2) fates provides the fundamental data to better

86   constrain the role of hydrolysis in modulating $_pON$ concentrations and lifetimes in the atmosphere, their

87   potential as a NO_x loss pathway, and their impacts on overall nitrogen budget, O_3 and SOA formation.

88

2. Methods

2.1. Chamber experiment design and procedure

A series of chamber experiments were performed in the Georgia Tech Environmental Chamber

facility (Boyd et al., 2015) housing two 12 m^3 Teflon reactors. Precursor volatile organic compounds (VOC)

were α-pinene (99 %, Sigma-Aldrich) and β-pinene (99 %, Sigma-Aldrich) and the oxidation conditions of

interest were hydroxyl and nitrate radical oxidation, which were represented as "daytime" and "nighttime"

experiments, respectively. Specifically, four different systems of VOC and oxidation conditions were

studied: α-pinene+OH, β-pinene+OH, α-pinene+NO$_3$, and β-pinene+NO$_3$. In order to infer the hydrolysis

process, experiments were performed under low RH (i.e., ~5 %) or high RH (i.e., ~50-70 %) conditions and

with effloresced or deliquesced seed particles for the same initial concentrations of precursor VOC and

oxidant precursors. Temperature in the reactors was kept at room temperature (22-25°C). Experimental

conditions are summarized in Table 1.

Prior to every experiment, the reactor was flushed with zero air (AADCO, 747-14) for at least a

day. A typical experiment began with the injection of seed aerosol into the reactor by atomizing dilute

ammonium sulfate (AS; 0.015 M) or sulfuric acid + magnesium sulfate (SA+MS; 0.01 + 0.005 M) aqueous

solution. The seed aerosol was either directly atomized into the reactor or passed through a dryer before

entering the reactor. The difference between efflorescence RH (~35 %) and deliquescence RH (~80 %) for

AS aerosol is fairly large (Seinfeld and Pandis, 2016). Taking advantage of this property, it is possible to

vary the amount of water in aerosol under the same RH in the reactor. Initial seed number and volume

concentrations upon atomization for 20 min were approximately 2×10^4 cm^{-3} and 2×10^{10} nm^3 cm^{-3},

respectively. A known amount of precursor VOC in the liquid form was transferred into a glass bulb, which

was then evaporated and carried into the reactor by flowing zero air at 5 L min^{-1} through the bulb. Although

the measurement of the precursor VOC concentration was not available for all experiments, the target and

measured concentrations in the experiments when the measurements were available were consistent.

113   For "daytime" experiments, an oxidant precursor (i.e., H_2O_2) was introduced to the reactor in the

114   same manner as VOC except that the glass bulb was gently heated by a heat gun to help evaporate faster.

115   During the injection of H_2O_2, a desired amount of NO was introduced into the reactor from a cylinder

116   containing 500 ppm NO (Matheson). For Exp. 3-5, 5 ppm NO at 5 L min^{-1} was continuously injected to the

117   reactor until the SOA growth ceased. For Exp. 1, 2, 6, and 7, 15 ppm NO at 5 L min^{-1} was injected for 5-

118   20 min several times until the SOA growth ceased. The NO concentration was usually on the order of tens

119   of ppb and always remained above a few ppb, making the bimolecular reaction with NO a favorable RO_2

120   reaction pathway. The experiment was initiated by turning on the irradiation of UV light approximately 20

121   min after the end of the last injection to ensure that particles and vapors were mixed well inside the reactor.

122   The procedure for "nighttime" experiments was the same until the end of the precursor VOC

123   injection. An oxidant precursor (i.e., N_2O_5) was pre-made in a flow tube by simultaneously injecting 500

124   ppm NO_2 (Matheson) at 0.4 L min^{-1} and ~250 ppm O_3 (Jelight 610) at 0.5 L min^{-1}. A simple kinetic box

125   model was used to adjust the concentration of O_3 and flow rates of both NO_2 and O_3 to maximize the

126   production of N_2O_5 and minimize the concentration of O_3, such that the VOC was dominantly oxidized by

127   nitrate radicals. Once N_2O_5 entered the reactor, it thermally decomposed to generate NO_2 and nitrate

128   radicals. VOC was usually depleted within the first 15 min of the experiment. For Exp. 8 and 14, the

129   injection order of precursor VOC and oxidant precursor was switched such that the injection of VOC

130   marked the beginning of the experiment. For Exp. 12 and 13, 25 ppm formaldehyde was added to the reactor

131   to enhance the branching ratio of $RO_2 + HO_2$ (Schwantes et al., 2015; Boyd et al., 2015) by injecting an

132   appropriate amount of formalin solution (37 % HCHO, Sigma-Aldrich) in the same manner as the injection

133   of H_2O_2. We do not discuss the details of the effect of the injection order nor the effects of the RO_2 fate

134   here as they had negligible impact on the results concerning hydrolysis.

135

136   2.2. Instrumentation and data analysis

137   A High Resolution Time-of-Flight Aerosol Mass Spectrometer (HR-ToF-AMS; Aerodyne

138   Research Inc.) measured the concentrations of non-refractory organics (Org), sulfate (SO_4), nitrate (NO_3),

139   ammonium (NH_4), and chloride (Chl) (DeCarlo et al., 2006). The data were analyzed using PIKA v1.16I.

140   For the majority of nitrate-containing aerosol regardless of the class (i.e., inorganic or organic), the nitrate

141   moiety (i.e., $-NO_2$, $-ONO_2$, and $-O_2NO_2$) was known to be thermally fragmented into NO^+ and NO_2^+ and

142   was measured as NO_3 (Farmer et al., 2010). As many past studies have demonstrated the feasibility to

143   separate the contribution of inorganic ($NO_{3,Inorg}$) and organic nitrate ($NO_{3,Org}$) to the measured NO_3 based

144   on the ratio of NO^+ and NO_2^+ (Fry et al., 2009; Farmer et al., 2010; Xu et al., 2015b; Kiendler-Scharr et al.,

145   2016; Fry et al., 2018), we used Eq. (1) presented in Farmer et al (2010) to obtain $NO_{3,Org}$. R_{AN} (i.e.,

146   NO^+/NO_2^+ from ammonium nitrate) was obtained from the routine ionization efficiency calibration of HR-

147   ToF-AMS using 300 nm ammonium nitrate particles. The drawback of this method is that R_{ON} (i.e.,

148   NO^+/NO_2^+ from organic nitrate aerosol) could vary depending on the chemical composition (Xu et al.,

149   2015b). In addition, a non-negligible contribution of ammonium nitrate could be expected in experiments

150   with deliquesced seed aerosol owing to high solubility of HNO_3. Thus, we obtained the R_{ON} measured in

151   low RH experiments for each system of VOC and oxidation condition. In order to account for changes in

152   R_{AN} over time, R_{ON} was scaled accordingly assuming that the ratio of R_{ON} to R_{AN} in the same system was

153   constant (Fry et al., 2013). R_{AN}, R_{ON}, and R_{ON}/R_{AN} values obtained in this study were consistent with

154   previously reported values (Fry et al., 2009; Bruns et al., 2010; Boyd et al., 2015; Nah et al., 2016) and are

155   summarized in Table S1.

156   A Filter Inlet for Gases and AEROsols (FIGAERO) (Lopez-Hilfiker et al., 2014) coupled to a High

157   Resolution Time-of-Flight Iodide Chemical Ionization Mass Spectrometer (HR-ToF-I-CIMS; Aerodyne

158   Research Inc.) detected a suite of gaseous and particulate oxidized organic species as well as selected

159   inorganic species (Bertram et al., 2011; Lee et al., 2014). The operation of FIGAERO-HR-ToF-I-CIMS

160   was detailed in the previous studies (Nah et al., 2016; Sanchez et al., 2016). Reagent ions were generated

161   by flowing a mixture of CH_3I and dry ultra high purity (UHP) N_2 (Airgas) through a polonium-210 source

162   (NRD; Model P-2021). The instrument measured gaseous compounds by sampling air from the reactor at

163   ~1.7 L min^{-1} while collecting particles onto a Teflon filter. Upon completion of the collection period,

164   collected particles were desorbed by temperature-programmed dry UHP N_2 flow and subsequently analyzed

165   by HR-ToF-I-CIMS. Sensitivity could decrease if the amount of reagent ions were significantly depleted

166   and/or if the secondary chemistry in the ion-molecule reaction (IMR) chamber occurred at a significant

167   degree (Lee et al., 2014). To avoid changes in sensitivity among experiments, gas-phase sampling flow was

168   diluted with zero air immediately before the inlet such that the evaporation of aerosol was minimal. The

169   amount of aerosol collected on the filter was also adjusted by varying the sampling rate from 1 to 6 L min^{-1}

170   depending on the aerosol mass concentrations inside the reactor. Overall, the fraction of reagent ions to

171   the total ions was kept above 80 %. In addition, iodide ion chemistry has been known to be affected by the

172   water vapor pressure inside the IMR owing to the difference in thermodynamics between I^- and IH_2O^- to

173   analyte compounds (Lee et al., 2014). In order to minimize changes in the water vapor pressure inside the

174   IMR, a small continuous flow of humidified UHP N_2 (30-50 ccm) through a bubbler at a reduced pressure

175   was continuously added to the IMR directly. Therefore, while the instrument was not calibrated to report

176   the concentration of detected species, it was possible to quantitatively compare measured signal of each ion

177   among experiments because the instrument was operated under configurations that prevented undesired

178   changes in sensitivity. The data were analyzed using Tofware v2.5.11 and all the masses presented in this

179   study were I^- adducts.

180   A Scanning Mobility Particle Sizer (SMPS) that consisted of a Differential Mobility Analyzer (TSI

181   3040) and a Ccondensation Particle Counter (TSI 3775) was operated under the low flow mode with the

182   sheath flow of 2 L min^{-1} to detect particles up to 1 μm in electrical mobility size. A Cavity Attenuated Phase

183   Shift spectroscopy (CAPS; Aerodyne Research Inc.) (Kebabian et al., 2005), an ultra-sensitivity NO_x

184   analyzer (Teledyne M200EU), and an UV absorption O_3 analyzer (Teledyne T400) measured NO_2, NO_x,

185   and O_3, respectively. In selected experiments, a Gas Chromatograph coupled to Flame Ionization Detector

186   (GC-FID; Agilent) was used to make sure that a desired amount of a precursor VOC was injected. Except

187   CAPS, NO_x analyzer, and O_3 analyzer, all instruments had their own dedicated sampling line.

188

189   **3. Results and discussion**

190   3.1. Chemical composition of secondary organic aerosol

191   Shown in Fig. 1 are the mass spectra of particle-phase species obtained from FIGAERO-HR-ToF-

192   I-CIMS at peak SOA growth. Many of the major species detected in this study are previously reported using

193   the same or different technique (Eddingsaas et al., 2012; Claflin and Ziemann, 2018; Boyd et al., 2015; Nah

194   et al., 2016; Lee et al., 2016; Romonosky et al., 2017). Concerning the chemical composition of SOA from

195   each system, a more distinct difference is observed between different oxidation conditions (i.e., hydroxyl

196   vs. nitrate radical oxidation) than between different precursor VOC (i.e., α-pinene vs. β-pinene). This is

197   expected as α-pinene and β-pinene have the same chemical formula and very similar structures while the

198   oxidation condition is distinctively different (Kroll and Seinfeld, 2008; Ziemann and Atkinson, 2012).

199   For "daytime" experiments where hydroxyl radicals are the dominant oxidants, the contribution of

200   ON (i.e., $C_xH_yN_{1,2}O_z$) and non-nitrated organics (i.e., $C_xH_yO_z$) are comparable and their contributions are

201   well spread out over a wide range of masses. A large contribution of $C_xH_yO_z$ is expected because the

202   formation of ON is a minor pathway in RO_2+NO (Perring et al., 2013). In Eddingsaas et al. (2012), the

203   major compounds reported in the α-pinene+OH system include $C_8H_{12}O_{4-6}$ and $C_{10}H_{16}O_{4,6}$, which are also

204   detected in our study. A suite of C_{10} ON from the chamber experiment of the α-pinene+OH system are

205   reported in Lee et al. (2016) with the chemical formula of $C_{10}H_{15,17,19}NO_{4-9}$. All of these masses are detected

206   in this study, though we observe a considerable contribution of $C_{<10}$ ON (i.e., $C_7H_{9,11}NO_6$ and

207      $C_9H_{13,15,17}NO_6$) as well as a small fraction of C_{10} dinitrate (i.e., $C_{10}H_{14,16}N_2O_{9,10}$) that has been rarely reported

208   (Fig. 1a). This significant contribution from species containing $C_{<10}$ indicates the large contribution of

209   fragmentation process that is a preferred pathway in high NO conditions (Kroll and Seinfeld, 2008;

210   Ziemann and Atkinson, 2012; Perring et al., 2013). It is possible that these species with $C_{<10}$ are thermally

211   decomposed products during the thermal desorption process (Stark et al., 2017). However, it is unlikely

212   that thermal decomposition plays a significant role for the SOA generated via hydroxyl radical oxidation

213   of monoterpenes because the desorption temperature for these compounds (i.e., peaking at ~50-70 ºC) are

214   much lower than the temperature at which decarboxylization or dehydration reactions (>120 ºC) are

215   expected to occur (Stark et al., 2017). SOA chemical composition of the β-pinene+OH system is similar to

216   that of the α-pinene+OH system but with a larger contribution of $C_xH_yO_z$.

217   Another interesting observation in the α-/β-pinene+OH systems is that a selected class of

218   compounds (i.e., $C_{10}H_{13,15,17}NO_{5-8}$) with the same H/C exhibit the same the time evolutions regardless of

219   the number of oxygen (Fig. S1). This observation is consistent with the autoxidation mechanism, in which

220   highly oxidized molecules are formed in a short time scale (Ehn et al., 2014; Crounse et al., 2013; Jokinen

221   et al., 2015). The detection of compounds with $O_{>7}$ also supports the presence of autoxidation process;

222   otherwise it is extremely difficult to produce highly oxidized molecules in a timescale of a few hydroxyl

223   radical oxidation reactions. It is important to note that the concentration of NO in our experiments has been

224   mostly kept on the order of tens of ppb over the course of the experiments by a continuous injection of

225   dilute NO and, therefore, this result suggests that autoxidation is not a negligible pathway of RO_2 fate even

226   at a moderately high NO level in laboratory experiments and in polluted ambient environments. Indeed,

227   recent studies (Berndt et al., 2016; Xu et al., 2019; Pye et al., 2019) suggest that the autoxidation rate

228   constant for the α-pinene+OH system could be up to a few per second, which is comparable to the NO level

229   of ~10 ppb. The autoxidation rate constant as well as the role of NO in autoxidation based on this

230   observation will be discussed in details in a forthcoming publication.

231   In contrast, the signals of $C_xH_yN_{1-2}O_z$ are dominant in the nitrate radical oxidation condition,

232   indicating that the production of ON is greatly favored over non-nitrated organics. This observation is

233   consistent with a direct addition of a nitrate functional group to a double bond (Wayne et al., 1991; Ng et

234   al., 2017), whereas the formation of ON in the hydroxyl radical oxidation condition is a minor channel of

235   RO_2+NO reaction (Perring et al., 2013). Moreover, the contribution from species containing $C_{<10}$ is

236   minimal. This is because unlike hydroxyl radical oxidation, a hydrogen subtraction reaction by a nitrate

237   radical is less efficient and, thus, multi-generation oxidation is unlikely to occur within the timescale of

238   experiments (Wayne et al., 1991; Ng et al., 2017). This means that once the precursor VOC undergoes

239   functionalization upon the initial nitrate radical oxidation, it is not likely to experience fragmentation during

240   the experiment. Unlike "daytime" SOA, the distribution of masses is dominated by a few signature ions,

241   such as $C_{10}H_{15}NO_{5,6}$ and $C_{20}H_{32}N_2O_{8-10}$ (Fig. 1c and 1d). In Boyd et al. (2015), Nah et al. (2016), and Lee

242   et al. (2016), the major species reported in the α-/β-pinene+NO_3 systems are monomeric nitrate aerosol

243   (i.e., $C_{10}H_{13,15,17,19}NO_{4-10}$), while in this study a substantial contribution of dimeric species (i.e., $C_{20}H_{32}N_2O_{8-}$

244    $_{11}$) is observed. The abundant presence of dimeric compounds has been previously observed in some studies

245   on nitrate radical oxidation of α-/β-pinene (Romonosky et al., 2017; Claflin and Ziemann, 2018) and

246   particle-phase reactions to produce such dimers have been proposed by Claflin and Ziemann (2018). Many

247   of the reported species in Claflin and Ziemann (2018) except the trimeric species (mass scan range not

248   extended to trimeric species in our study) are observed in our study. One major difference between Claflin

249   and Ziemann (2018) and this study is the substantial presence of monomeric nitrate aerosol (i.e., 30-60 %

250   by signal) in this study. This difference may be attributed to the difference in the amount of available

251   monomeric blocks to form dimer species. Assuming reversible dimerization process, the concentration of

252   dimer species shall be proportional to the square of monomer concentration, such that the monomer to

253   dimer ratio increases in a quadratic manner as the available monomer concentration decreases. Since the

254   amount of SOA formed in Claflin and Ziemann (2018) is approximately two orders of magnitude higher

255   than that in this study, the concentration of monomers in the particle-phase is higher, favoring a more

256   efficient formation of dimeric species. Together, these results suggest that the contribution of dimeric nitrate

257   aerosol could vary greatly depending on the concentrations of monomeric blocks at the specific time and

258   location.

259   Previous field studies have reported the mass spectra of ambient C_{10} $_pON$ obtained by FIGAERO-

260   HR-ToF-I-CIMS in rural Alabama site during the Southern Oxidant and Aerosol Study (SOAS) (Lee et al.,

261   2016) and in rural forest in Germany (Zhang et al., 2018). A comparison of the ambient mass spectra with

262   those obtained in this study reveals that average ambient $_pON$ resembles "daytime" $_pON$ more than

263   "nighttime" $_pON$ (Fig. S2). $_pON$ from "daytime" experiments has a distribution of masses centered around

264    $C_{10}H_{13,15,17}NO_7$, which is consistent with the ambient measurement data. On the other hand, nitrate radical

265   oxidation does not seem to oxidize organic species enough that the distribution of masses is skewed towards

266   a less-oxidized region (i.e., $C_{10}H_{13,15,17}NO_{5-6}$). However, it is difficult to draw a quantitative conclusion

267   simply based on this comparison because O_3, another important oxidant at night, is not studied. Moreover,

268   an average lifetime of aerosol could extend up to a week and thus ambient aerosol is continuously exposed

269   to further oxidation while the experiments here are more applicable to freshly formed aerosol. In addition,

270   the use of C_{10} $_pON$ alone may not be a good representative of monoterpene-derived $_pON$ as 42-74 % of $_pON$

271   in this study contains fewer or more than 10 carbon (Table S2). Nonetheless, the chemical composition of

272   aerosol generated in this study is comparable to those in the atmosphere and, thus, the results shall be

273   directly applicable to relevant ambient conditions.

274

275   3.2. Hydrolysis of particulate organic nitrate

276   3.2.1. Proxy used to evaluate hydrolysis process

277   Various proxies using HR-ToF-AMS data have been used to infer ON hydrolysis in previous

278   studies. In Bean and Hildebrandt Ruiz (2016), NO_3 measured by an Aerosol Chemical Speciation Monitor

279   (ACSM, practically similar to how AMS operates and measures aerosol species) (Ng et al., 2011) is

280   normalized to SO_4 as a means to account for particle wall-loss and is fitted by an exponential function to

281   estimate the ON hydrolysis rate. On the other hand, Boyd et al. (2015) normalize NO_3 measured by HR-

282   ToF-AMS to Org and attribute the relative decay of NO_3/Org between humid (RH ~50 %) to dry (RH <5

283   %) conditions to hydrolysis. Other approaches include the SMPS-derived particle wall-loss correction of

284   NO_3 measured by HR-ToF-AMS followed by fitting its decay trend (Liu et al., 2012b) and the determination

285   of fraction of total (i.e., gas and particle) ON to the precursor VOC consumed as a function of RH using a

286   Fourier-Transform InfraRed spectroscopy (FTIR). Below, we systematically examine the use of different

287   proxies using HR-ToF-AMS data to infer hydrolysis and discuss how the corresponding results are

288   interpreted.

289   Figure 2 shows the time series of Org, NO_3, SO_4, and NH_4 measured by HR-TOF-AMS for α-

290   pinene+NO_3 system. There is a substantial difference in NO_3 for the same VOC system but under different

291   reactor RH and phase state of seed particles (Exp. 10 and 11), while Org and SO_4 concentrations are similar.

292   The spike in NO_3 in high RH wet seed experiment (Fig. 2b) is attributed to the uptake of N_2O_5 and/or

293   dissolution of HNO_3 into aqueous aerosol followed by neutralization with ammonia to produce ammonium

294   nitrate. This is consistent with the sharp increase in molar ratio of NH_4/SO_4 to higher than 2, which is the

295   theoretical value for AS particles. It is also possible that inorganic nitrate is generated via hydrolysis of

296   gaseous ON that is too volatile to condense but is soluble enough to dissolve in aqueous aerosol and, thus,

297   only appears in high RH experiments. Since we do not have a way to quantitatively differentiate the

298   contribution of the aforementioned sources, the focus of this study is on hydrolysis of $_pON$ that is condensed

299   driven by volatility. However, further study is required to investigate the hydrolysis of volatile yet soluble

300   gaseous ON, and the approach must be different from the comparison between low and high RH

301   experiments to obtain meaningful results.

302   To evaluate the extent of $_pON$ hydrolysis, the contributions of inorganic nitrate ($NO_{3,Inorg}$) and

303   organic nitrate ($NO_{3,Org}$) to the measured NO_3 need to be calculated. Firstly, $NO_{3,Org}$ is estimated by

304   subtracting NO_3 associated with excess NH_4. Secondly, $NO_{3,Org}$ is derived from NO^+/NO_2^+ approach (Sect.

305   2.2.). Figure S3 shows the comparison of $NO_{3,Org}$ estimated by these two independent methods for the α-

306   pinene+NO_3 system. It is clear that $NO_{3,Org}$ from both methods are consistent and that there is a considerable

307   contribution of $NO_{3,Inorg}$ to NO_3 in the experiment. We note the contribution of $NO_{3,Inorg}$ to NO_3 can vary

308   depending on experimental conditions with a range from to 28 to 90 % for all experiments in this study.

309   Nevertheless, these results demonstrate that for laboratory experiments with high RH and wet seeds, when

310   using HR-ToF-AMS data to infer hydrolysis, it is important to separate the measured NO_3 into $NO_{3,Inorg}$ and

311    $NO_{3,Org}$.

312   Once NO_3 is separated into $NO_{3,Inorg}$ and $NO_{3,Org}$, we evaluate whether the normalization of $NO_{3,Org}$

313   to SO_4 and Org provides a consistent decay trend. Photooxidation of α-pinene (Exp. 3-5) is used as a case

314   system. As hydrolysis is a reaction where liquid water is directly involved in, it is expected that the rate of

315   hydrolysis will change proportionally as a function of aerosol water content. Based on the hygroscopicity

316   parameter for AS ($\kappa = 0.53$) (Petters and Kreidenweis, 2007) and for ambient LO-OOA ($\kappa = 0.08$) (Cerully

317   et al., 2015) that has a substantial contribution from $_pON$ (Xu et al., 2015a), estimated aerosol water contents

318   at peak SOA growth in Exp. 3-5 are approximately 0, 1, and 26 $\mu g\ m^3$, respectively. Figure S4 illustrates

319   that AS seed particles are indeed effloresced in Exp. 4 (high RH, dry AS) but not in Exp. 5 (high RH, wet

320   AS). These mass concentrations of aerosol water translate to 0, 6, and 36 mol L^{-1}, respectively, under the

321   assumption that SOA is miscible with liquid water. It is speculated that SOA formed in Exp. 3-5 are miscible

322   with water because (1) the measured O/C ratio in HR-ToF-AMS (Canagaratna et al., 2015) is close to 0.7,

323   which is near the lower end but above the liquid-liquid phase separation condition (Song et al., 2012) and

324   (2) there is evidence of aqueous-phase reactions which highly depend on the availability of aerosol water,

325   as discussed in Sect. 3.3. Thus, the decay rate of $NO_{3,Org}$ normalized to SO_4 and/or Org between Exp. 4 and

326   Exp. 5 shall differ by a factor of 6 based on the molar concentrations of aerosol water.

327   Figure 3a shows the mass ratio of $NO_{3,Org}/SO_4$ and the decay rate as a characteristic time in Exp. 3-

328   5. The characteristic times of Exp. 4 and 5 (4.4 vs. 4.0 h) do not differ regardless of the molar concentrations

329   of aerosol water, suggesting that the decreasing trend in $NO_{3,Org}/SO_4$ may not be due to changes in aerosol

330   water content and $_pON$ hydrolysis, but arise from the difference in the reactor humidity alone. A comparison

331   of $NO_{3,Org}/SO_4$ and $NO_{3,Org}/Org$ also reveals that these two proxies capture a different range of decay

332   mechanisms. Figure 3b shows the relative decay trend of $NO_{3,Org}/SO_4$ and $NO_{3,Org}/Org$ between Exp. 4 (high

333   RH) and Exp. 3 (low RH). If hydrolysis is a dominant decay mechanism of $_pON$, the trend of $NO_{3,Org}/Org$

334   would be identical to that of $NO_{3,Org}/SO_4$. This is because the organic moiety of hydrolysis product is

335   generally considered to have a substituted alcohol group (Boschan et al., 1955) and to have a relatively

336   similar vapor pressure and shall remain in the particle phase (Pankow and Asher, 2008). However, the

337   measured decay trend of the two proxies is greatly different. It is possible that some organic moiety of

338   hydrolysis product could be significantly more volatile and repartition back to the gas phase (Rindelaub et

339   al., 2016; Bean and Hildebrandt Ruiz, 2016) and, thus, both organics and HNO_3 formed from hydrolysis

340   evaporate. In this case, not only $NO_{3,Org}$ but also some fraction of Org would decrease because Org measured

341   by HR-ToF-AMS includes the contribution from the organic part of $_pON$. This will lead to the relatively

342   smaller decrease in $NO_{3,Org}$/Org compared to $NO_{3,Org}$/SO_4. We can reconstruct the decay rate of $NO_{3,Org}$/Org

343   assuming 1) the decay rate of $NO_{3,Org}$/SO_4 is solely due to hydrolysis of $_pON$ and 2) the maximum

344   contribution of $_pON$ to OA is 35 % (see Fig. 4 and discussions below). The reconstructed decay rate of

345      $NO_{3,Org}$/Org is shown in Fig. 3b. As observed in the figure, the decay rate of the reconstructed $NO_{3,Org}$/Org

346   is much larger than the measured $NO_{3,Org}$/Org. This suggests that hydrolysis is not the only loss process

347   reflected in the decreasing trend of $NO_{3,Org}$/SO_4, while $NO_{3,Org}$/Org is likely a better proxy that isolates

348   hydrolysis from other loss processes. The likely important loss process manifested in $NO_{3,Org}$/SO_4 is the

349   loss of organic vapors to the walls of the rector (Matsunaga and Ziemann, 2010; Krechmer et al., 2016;

350   Huang et al., 2018; Loza et al., 2010; Mcvay et al., 2014; Zhang et al., 2015; Zhang et al., 2014; La et al.,

351   2016). For example, Huang et al. (2018) observe that the decay of isoprene hydroxyl nitrate depends on the

352   reactor humidity. Therefore, $NO_{3,Org}$/Org is a better proxy to infer hydrolysis of $_pON$ than others.

353

354   3.2.2. Hydrolysis lifetime of particulate organic nitrate

355   In order for the data to be easily comparable with those reported in models or using other technique,

356   the use of general terms instead of the AMS specific terms (i.e., $NO_{3,Org}$ and Org) can be convenient. We

357   define $_pON$ as the total mass concentration of particulate organic nitrate (includes organics part and nitrate

358   part of the ON compounds) and OA as the total mass concentration of organic aerosol (includes nitrate and

359   non-nitrated organics). The inclusion of nitrate mass in OA is important as the contribution of nitrate

360   functional groups to the total organic aerosol concentration is large. The conversion method from

361      $NO_{3,Org}$/Org into $_pON$/OA is illustrated in Eq. (1).

$$\frac{_pON}{OA} = \left(\frac{\frac{NO_{3,Org}}{Org}}{1 + \frac{NO_{3,Org}}{Org}} \right) * \left(\frac{MW_{_pON}}{MW_{NO_3}} \right) \qquad (1)$$

362   MW_{pON} represents the average molecular weight of $_pON$ per nitrate functional group estimated from

363   FIGAERO-HR-ToF-I-CIMS data, and MW_{NO3} indicates the molecular weight of nitrate (i.e., 62 g mol^{-1}).

364   Since MW_{pON} does not significantly vary during the course of experiments (i.e., relative standard deviation

365   of <1.2 %), the average value is applied to each experiment. The variability of MW_{pON} among different

366   systems is also found to be small, ranging from 229 to 238 g mol^{-1} and, thus, an average MW_{pON} is used for

367   experiments where FIGAERO-HR-ToF-I-CIMS data are not available. Figure 4 shows the time-series data

368   of $_pON/OA$ for all the systems investigated in this study.

369   For "nighttime" experiments, the relative ratio of $C_xH_yN_{1-2}O_z$ and $C_xH_yO_z$ obtained from

370   FIGAERO-HR-ToF-I-CIMS data in Fig. 1 does not appear to match well with $_pON/OA$ from HR-ToF-

371   AMS data. For example, the signals are dominated by $C_xH_yN_{1-2}O_z$ in the β-pinene+NO$_3$ system, as shown

372   in Fig. 1d, while $_pON/OA$ is at most 0.5, as shown in Fig. 4d. The discrepancy would be attributed to the

373   overestimation of Org (in particular, C_xH_y family) in HR-ToF-AMS and/or underestimation of $C_xH_yO_z$ in

374   FIGAERO-HR-ToF-I-CIMS. Relative ionization efficiency (RIE) of less-oxidized organic species in HR-

375   ToF-AMS is experimentally measured to be higher at least by a factor of 2 (Xu et al., 2018b). As previously

376   reported (Boyd et al., 2015), the HR-ToF-AMS mass spectrum of SOA formed from β-pinene+NO$_3$

377   contains significant amounts of C_xH_y fragments, indicating the less-oxidized nature of SOA from β-

378   pinene+NO$_3$. For example, if the true RIE of Org by β-pinene+NO$_3$ SOA were to be a factor of 2 higher

379   than the default RIE of Org (i.e., 1.4), the reported concentration of Org would have been overestimated by

380   a factor of 2, such that actual $_pON/OA$ would have been higher than reported in Fig. 4d. On the other hand,

381   an iodide reagent ion is not quite selective to detect less oxidized species, which could overestimate the

382   contribution of $_pON$ to OA (Aljawhary et al., 2013). Nonetheless, this discrepancy between HR-ToF-AMS

383   and FIGAERO-HR-ToF-I-CIMS data, however, should not affect the results regarding the hydrolysis

384   lifetime and hydrolyzable fraction of $_pON$ presented later.

385   As illustrated in Fig. 4, the time series of $_pON/OA$ stabilizes fairly quickly in most of the

386   experiments, regardless of RH and/or the phase state of seed aerosol. This suggests that the timescale of

387    $_pON$ hydrolysis in the systems studied is significantly shorter or longer than the timescale of our

388   experiments. It is also evident from Fig. 4 that $_pON/OA$ in high RH experiments are always lower than that

389   in low RH experiments. These two observations imply that the rate of $_pON$ hydrolysis may be fast enough

390   that the decay trend of $_pON$ compared to OA is not visibly manifested, though a clear difference of $_pON/OA$

391   between low and high RH experiments is exhibited as a result of fast hydrolysis. Since no sudden, drastic

392   change in $_pON/OA$ is observed except for a few initial data points, we conclude that the hydrolysis lifetime

393   of hydrolyzable $_pON$ for α-/β-pinene derived ON shall be no more than 30 min (i.e., 3 data points in Fig.

394   4). Particle acidity is found to enhance the rate of hydrolysis in prior study (Rindelaub et al., 2016), though

395   no clear difference is observed between experiments with AS and SA+MS seed particles (i.e., Exp. 5 and

396   2). $_pON$ formed from hydroxyl and nitrate radical oxidation of α-pinene and β-pinene may not require a low

397   pH to undergo hydrolysis at a rate comparable to the timescale of chamber experiments.

398   Comparing with the results from past chamber studies reporting a $_pON$ hydrolysis lifetime of 3 to

399   6 h (Liu et al., 2012b; Bean and Hildebrandt Ruiz, 2016; Boyd et al., 2015), our estimated hydrolysis

400   lifetime is substantially shorter, but is consistent with the range (i.e., 1 min to 8.8 h) reported in studies

401   using the bulk solution (Darer et al., 2011; Hu et al., 2011; Jacobs et al., 2014; Rindelaub et al., 2016) (Fig.

402   5). In Liu et al. (2012) and Bean and Hildebrandt Ruiz (2016), the hydrolysis lifetime is derived from the

403   decay rate of NO_3 corrected for the particle wall loss or normalized to SO_4. As demonstrated in Sect. 3.2.1.,

404   this NO_3/ SO_4 decay rate is likely affected by other loss processes, such as vapor wall loss, and, thus, is not

405   a good proxy to estimate the hydrolysis lifetime. The apparent discrepancy does not stem from the

406   contradiction in the obtained data itself but rather in the data interpretation. Indeed, the lifetime estimated

407   based on the decay of $NO_{3,Org}/SO_4$ in our study is 4 h (Fig. 3a) that is consistent with 6 and 3 h reported in

408   Liu et al. (2012) and Bean and Hildebrandt Ruiz (2016). On the other hand, in Boyd et al. (2015) the

409   hydrolysis lifetime is estimated based on the decay rate of NO_3/Org. The discrepancy in the reported

410   hydrolysis lifetime here could be attributed to the fact that NO_3 is not separated into $NO_{3,Org}$ and $NO_{3,Inorg}$.

411   Figure S5 shows our data analyzed in the same manner as Boyd et al. (2015). The lifetime calculated based

412   on the decay is 2.2 h, which is close to the reported 3 h (Boyd et al., 2015). The reduction of NO_3/Org in

413   Fig. S5 (~30 %) is greater than in Boyd et al. (2015) (10 %), which could be because (1) the amount of

414   N_2O_5, a source of inorganic nitrate, used in our study is slightly larger and (2) RH in our study is higher by

415   10-20 %, which may have allowed greater uptake of N_2O_5 to produce inorganic nitrate.

416   In previous bulk solution studies where the concentration of interested organic nitrate (in particular

417   hydroxyl nitrate) in aqueous solution rather than in aerosol water is monitored over time, it is unlikely that

418   the data interpretation is affected by other loss processes present in chamber experiments, such as vapor

419   wall-loss. It is also common to monitor the organic moiety of hydrolysis product (Darer et al., 2011), while

420   it is extremely difficult in chamber experiments where hundreds of organic species are present at the same

421   time, leading to the difficulty in accurately measuring the hydrolysis lifetime in chamber experiments.

422   Based on the comprehensive analysis we demonstrate above on evaluating $_p$ON hydrolysis in chamber

423   experiments, we recommend the use of the hydrolysis lifetime reported in this study, which is no more than

424   30 min, for $_p$ON formed from α-pinene and β-pinene.

425

426   3.2.3. Hydrolyzable fraction of particulate organic nitrate

427   The fraction of hydrolyzable $_p$ON (F_H) can be directly estimated from the difference in $_p$ON/OA

428   between low and high RH experiments shown in Fig. 4. Although we show that hydrolysis is substantially

429   faster than the timescale of chamber experiments in our study, there still appears a clear difference in

430    $_p$ON/OA between high RH experiments but with a different phase state of seed aerosol (i.e., Exp. 4 and 5).

431   The difference mass spectra among Exp. 3-5 obtained from FIGAERO-HR-ToF-I-CIMS reveal that the

432   difference in $_p$ON/OA between Exp. 4 and 5 does not arise from the reduction in $_p$ON but from the increase

433   in non-nitrated organics (Fig. 6). The reason for this OA increase with the abundant presence of aerosol

434   water is speculated to be uptake and other aqueous-phase reactions than hydrolysis and is briefly discussed

435   in Sect. 3.3. Thus, the absolute difference in $_p$ON/OA between low RH, dry seed and high RH, dry seed

436   experiments best indicates F_H. Depending on the fate of the organic moiety of the hydrolysis product (i.e.,

437   stay in the particle phase or repartition back to the gas pahse), F_H varies. Since we are unable to determine

438   the fate of hydrolysis product, an upper and lower limit of F_H are reported as a range of F_H. For the α-

439   pinene+OH system, 23-32 % of $_p$ON formed undergoes hydrolysis within the timescale of the experiments.

440   For the other systems with no experiment under high RH with dry seed aerosol, the same level of additional

441   contribution from non-nitrated organics encountered in α-pinene+OH system is assumed and F_H is scaled

442   accordingly. For the β-pinene+OH, α-pinene+NO₃, and β-pinene+NO₃ systems, 27-34, 9-17, and 9-15 %

443   of $_pON$ are found hydrolyzable within the timescale of the experiments. Table 2 summarizes the hydrolysis

444   lifetime and F_H in the systems explored in this study.

445   F_H has been only reported in several studies (Liu et al., 2012b; Boyd et al., 2015; Zare et al., 2018).

446   The determination of F_H is essential because the assumption that all $_pON$ hydrolyzes biases the relative

447   importance of hydrolysis among the loss mechanisms of $_pON$ and NO_x. Boyd et al. (2015) report that F_H of

448    $_pON$ formed via β-pinene+NO₃ is ~10 %, which is in a good agreement with our range of 9-15 %. From a

449   perspective of predicted molecular structures of $_pON$, <5 % of $_pON$ from β-pinene+NO₃ are tertiary (Claflin

450   and Ziemann, 2018) that is expected to undergo hydrolysis in minutes (Darer et al., 2011; Hu et al., 2011).

451   In our study, a considerable contribution of monomeric (C_{10}) $_pON$ is observed (Fig. 1d), while dimeric (C_{20})

452    $_pON$ is dominant in Claflin and Ziemann (2018). This may indicate that monomeric $_pON$ is more susceptible

453   to hydrolysis such that F_H in this study is slightly higher than expected based on the proposed molecular

454   structures of $_pON$ in Claflin and Ziemann (2018).

455   F_H for α-/β-pinene+OH systems are higher than those from α-/β-pinene+NO₃ systems. This trend

456   is consistent with the understanding that $_pON$ via hydroxyl radical oxidation have a larger fraction of tertiary

457   nitrate groups, which are significantly more susceptible to hydrolysis (Darer et al., 2011; Hu et al., 2011)

458   than those formed via nitrate radical oxidation (Ng et al., 2017). Although the relative trend of F_H between

459   α-/β-pinene+OH and α-/β-pinene+NO₃ systems is consistent, the magnitude of F_H in the α-/β-pinene+OH

460   system appears to be smaller than expected based on the tertiary nitrate fraction estimated via the explicit

461   gas-phase chemical mechanism (Browne et al., 2013; Zare et al., 2018). In previous studies, F_H are

462   estimated to be 62 and 92 % for α-/β-pinene+OH systems, respectively. However, our results indicate F_H is

463   23-32 and 27-34 % for the same systems (Fig. 5). The chemical mechanism used in Browne et al. (2013)

464   and Zare et al. (2018) are based on the Master Chemical Mechanism (MCM) that is well known in the

465   degradation chemistry of VOC in the gas phase (Jenkin et al., 1997; Saunders et al., 2003). However, the

466   same mechanism performs poorly in regards to the chemical composition of SOA (Faxon et al., 2018) as

467   well as the prediction of SOA formation (Ruggeri et al., 2016; Boyd et al., 2017) when equipped with gas-

468   particle partitioning modules based on the absorptive gas-particle partitioning theory (Pankow, 1994). It is,

469   therefore, reasonable to argue that the chemical composition of $_p$ON could greatly differ from that of total

470   ON predicted by the MCM. Thus, F_H reported in this study provides the fundamental experimental

471   constraints on $_p$ON hydrolysis, that can be used in regional and global models for elucidating potential

472   impacts of ON on nitrogen budget and formation of ozone and aerosol.

473

474   3.3 Signature of other aqueous-phase reactions than hydrolysis

475   As briefly discussed in the above section, the presence of elevated level of aerosol water seems to

476   have enhanced the contribution of small (i.e., $C_{<9}$) but more-oxidized organic species to SOA. As shown in

477   Fig. 5c, the enhancement is observed for a variety of non-nitrated organic aerosol including $C_4H_{6,8}O_3$,

478     $C_4H_4O_4$, $C_5H_6O_5$, $C_7H_{8,10}O_4$, and $C_8H_{8,10}O_{4,5}$, while $_p$ON overall neither increase nor decrease. $C_5H_6O_5$ has

479   been reported as a product of the aqueous-phase reaction of α-pinene derived compounds (Aljawhary et al.,

480   2016). Other compounds, such as $C_4H_4O_4$, $C_7H_{8,10}O_4$, and $C_8H_{10}O_5$, also appear to result from the aqueous

481   processing because compounds with similar chemical formulae but with slightly higher degrees of oxidation

482   (i.e., $C_4H_4O_5$, $C_7H_{10}O_5$, and $C_8H_{12}O_6$) are reported in Aljwhary et al. (2016). The reason for this less

483   oxidized nature of SOA in this study may be attributed to our experiments being performed in moderately

484   high NO conditions that promotes a higher contribution of a carbonyl group than a hydroperoxyl group,

485   which is preferred in low NO conditions. In Aljwhary et al. (2016), the starting compound is a product in

486   low NO conditions (pinonic acid, $C_{10}H_{16}O_3$). Thus, it is reasonable that products of the aqueous processing

487   in this study are slightly less oxidized than observed in Aljwhary et al. (2016).

488   The enhancement of non-nitrated organic aerosol in FIGAERO-HR-ToF-I-CIMS may be due to

489   aqueous processing of species in the particles in the presence of aerosol water. This can come from further

490   reactions of semi/low-volatile species in the particle phase, or reactive uptake of volatile (but highly water-

491   soluble) species into the aerosol followed by subsequent aqueous-phase reactions to form low-volatility

492 products (Ervens et al., 2011). A comparison of the average thermogram at peak SOA growth among Exp.

493 3-5 indicates a higher contribution of low-volatility compounds in Exp. 5 than in Exp, 3 and 4, as illustrated

494 by the bimodal peaks (Fig. S6). Given the same degree of gas-phase oxidation expected among Exp. 3-5,

495 these results show that that aqueous chemistry in wet aerosol contributes to the further formation of low-

496 volatility compounds. Overall, the highest average degree of oxidation (O/C = 0.77) is observed in high RH

497 wet aerosol experiment (Expt. 5). The effect of particle water on monoterpene SOA formation warrants

498 further studies.

499

500 3.4 Atmospheric implications

501   There is emerging evidence that monoterpene SOA greatly contribute to atmospheric aerosol in the

502 Southeastern U.S. (Zhang et al., 2018; Xu et al., 2018a). ON is no exception; a substantial fraction of $_p$ON

503 is considered to be from monoterpenes (Lee et al., 2016; Huang et al., 2019; Xu et al., 2015a). While C_{10}

504 $_p$ON measured in FIGAERO-HR-ToF-I-CIMS is a good tracer of monoterpene derived $_p$ON, we show that

505 a fair amount of α-/β-pinene $_p$ON is found as $C_{<10}$ or C_{20} depending on the oxidation condition. This implies

506 that the contribution of monoterpene derived $_p$ON could be substantially underestimated when only

507 considering C_{10} $_p$ON. Fraction of $_p$ON with different number of carbon reported in this study (Table S2) is

508 a useful parameter to quantitatively determine the contribution of monoterpenes derived $_p$ON to total $_p$ON.

509   Many previous modeling studies using ambient measurement data as constraints report that the

510 lifetime of $_p$ON is likely several hours (Pye et al., 2015; Fisher et al., 2016; Lee et al., 2016; Zare et al.,

511 2018). Hydrolysis of $_p$ON is used as a dominant loss process with the lifetime of several hours to improve

512 the concentration of modeled OA (Pye et al., 2015) and to improve the concentrations of gaseous and

513 particulate ON (Fisher et al., 2016). If the ambient $_p$ON concentration is indeed governed by a loss process

514 with a few hours of lifetime, our results imply that the particle-phase hydrolysis may not be the only

515 dominant loss process because the hydrolysis lifetime reported in this study is significantly shorter. Other

516 potential but less-studied loss mechanisms of ON and $_p$ON include deposition (Nguyen et al., 2015),

517 photolysis (Muller et al., 2014), and aqueous photooxidation (Romonosky et al., 2017; Nah et al., 2016).

518 For instance, enhanced photolysis rate is observed for carbonyl nitrate derived from isoprene (Muller et al.,

519 2014), while no similar study is available for monoterpene derived ON in literature. Also, it has been

520 demonstrated that different monoterpene $_pON$ can have drastically different photochemical fates (Nah et

521 al., 2016). Taken together, results from this study highlight the importance to investigate other potential

522 loss processes of monoterpene derived $_pON$.

523 Aside from the hydrolysis lifetime, many modeling studies assume F_H as unity (Pye et al., 2015;

524 Fisher et al., 2016; Lee et al., 2016). Even when F_H is considered, the value of F_H used in other studies is

525 still substantially higher than estimated in this study (Browne et al., 2013; Zare et al., 2018). The use of

526 higher F_H would result in overestimating the contribution of hydrolysis as a loss process of $_pON$ and NO_x.

527 While hydrolysis is considered as a permanent sink of NO_x, many other loss processes, such as further

528 hydroxyl radical oxidation and photolysis, are considered as a temporary reservoir of NO_x. If the relative

529 importance of $_pON$ fates in models was not accurate, the role of ON in NO_x cycling and the formation

530 potential of ozone could have been inaccurately interpreted. Therefore, results from this study regarding

531 the hydrolysis lifetime and F_H serve as experimentally constrained parameters for chemical transport

532 models to accurately evaluate the role of ON in regards to nitrogen budget and the formation of ozone and

533 fine aerosol.

534

535 **Author contribution**

536 M.T. designed and performed the research and analyzed the data with substantial inputs from N.L.N. M.T.

537 and N.L.N. wrote the manuscript.

538

539 **Acknowledgements**

540 The authors would like to acknowledge financial support by National Science Foundation (NSF) CAREER

541 AGS-1555034 and by National Oceanic and Atmospheric Administration (NOAA) NA18OAR4310112.

542 The FIGAERO-HR-ToF-CIMS has been purchased through NSF Major Research Instrumentation (MRI)

543 Grant 1428738.

545
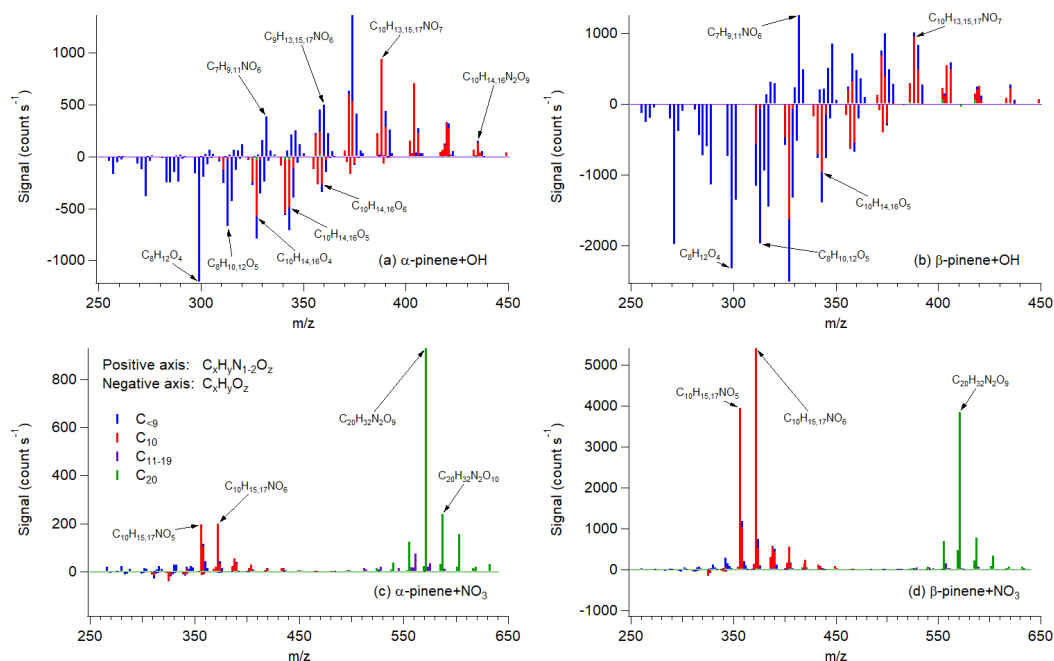
Figure 1. FIGAERO-HR-ToF-I-CIMS mass spectra of SOA in (a) α-pinene+OH from Exp. 3, (b) β-

pinene+OH from Exp. 6, (c) α-pinene+NO₃ from Exp. 10, and (d) β-pinene+NO₃ from Exp. 14. Top portion

of each panel represents $C_xH_yN_{1-2}O_z$, whereas bottom represents $C_xH_yO_z$. Bars are colored by the number

of carbon as noted in the legend. Prominent masses are labeled with the corresponding chemical formulae

without an iodide ion.

551

552
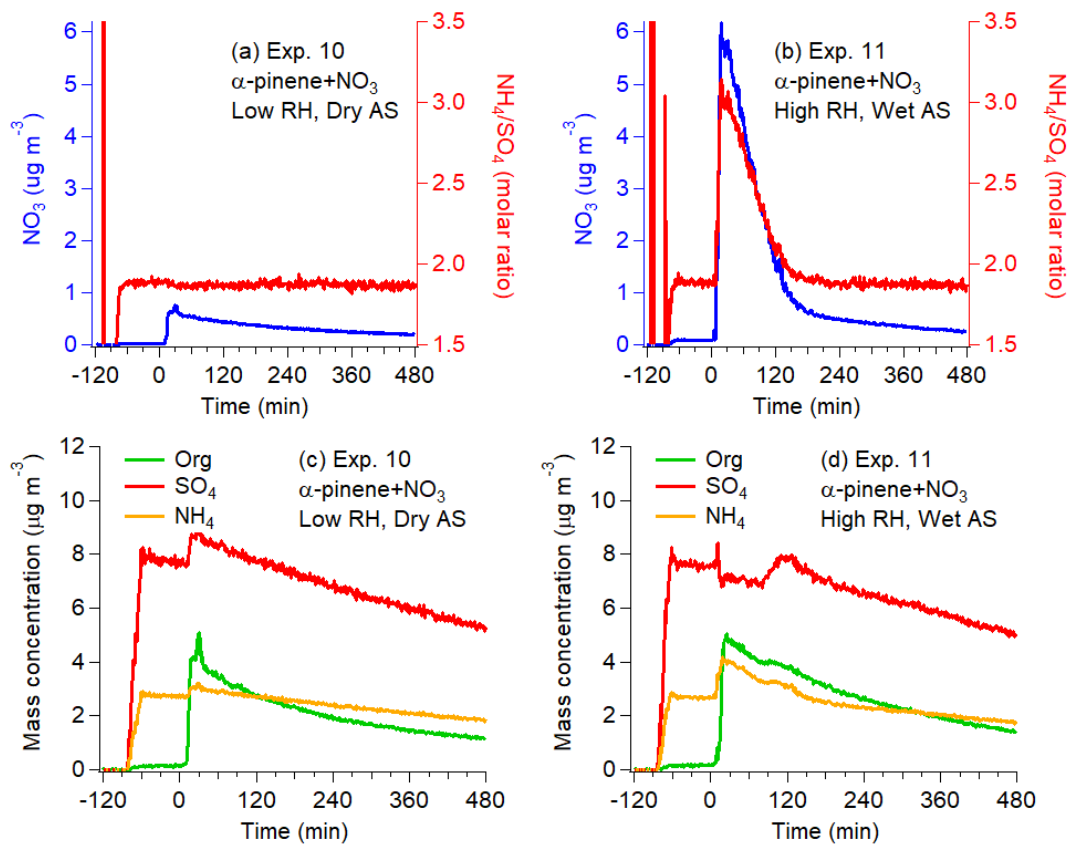
Figure 2. (a, b) NO_3 concentration and the molar ratio of NH_4 to SO_4 and (c, d) concentrations of Org, SO_4,

and NH_4 measured by HR-ToF-AMS. Data presented in Panels (a) and (c) are from Exp. 10 (low RH, dry

AS), while those in Panels (b) and (d) are from Exp. 11 (high RH, wet AS). These two experiments are

essentially the same except for RH and phase state of seed aerosol.

557

558
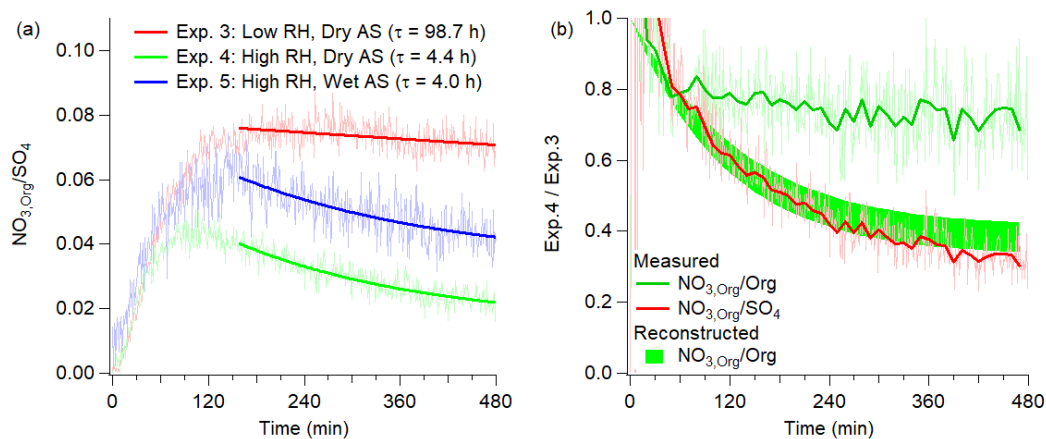
Figure 3. (a) Time-series data of $NO_{3,Org}/SO_4$ from Exp. 3-5 (α-pinene+OH) and the exponential fits with

559

corresponding characteristic times. (b) $NO_{3,Org}/Org$, $NO_{3,Org}/SO_4$, reconstructed $NO_{3,Org}/Org$ based on the

560

decay rate of $NO_{3,Org}/SO_4$.

561

562
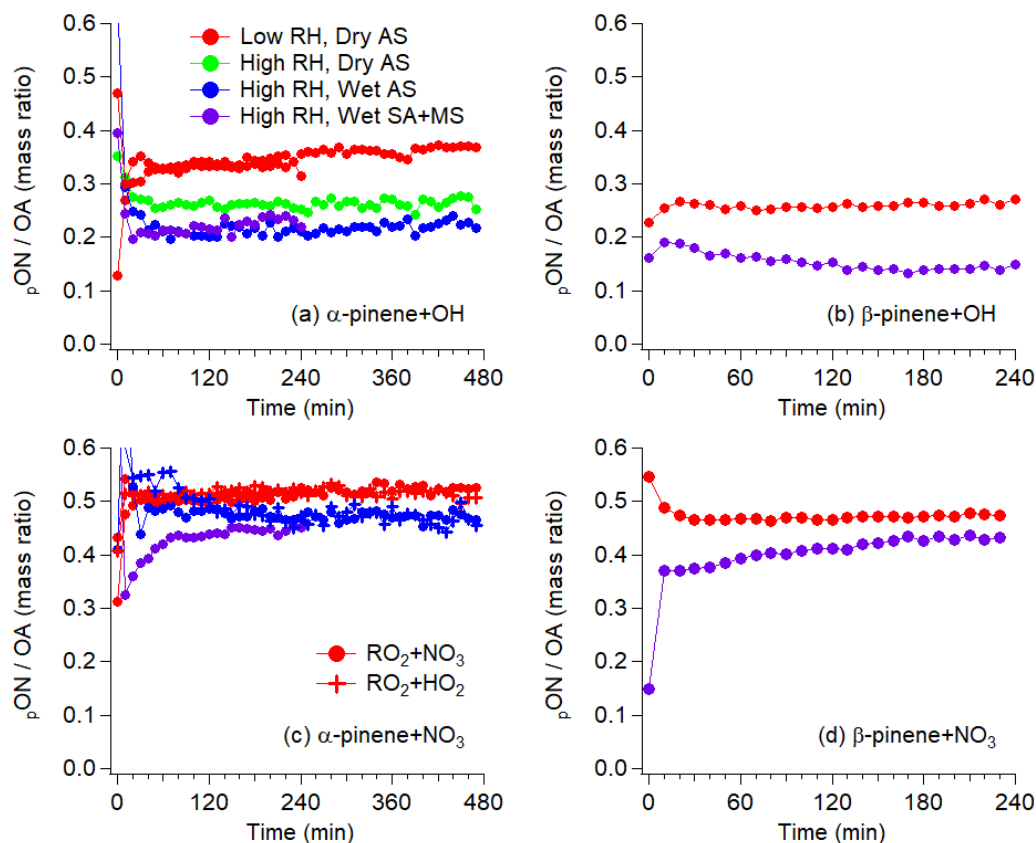
Figure 4. Time-series data of $_pON/OA$ in (a) α-pinene+OH from Exp. 1-5, (b) β-pinene+OH from Exp. 6-

7, (c) α-pinene+NO$_3$ from Exp. 8-13, and (d) β-pinene+NO$_3$ from Exp. 14-15. Data points are colored by

conditions concerning reactor RH and phase state of seed aerosol. For α-pinene+NO$_3$, data points are also

shaped differently depending on the expected dominant RO$_2$ fate.

567

568
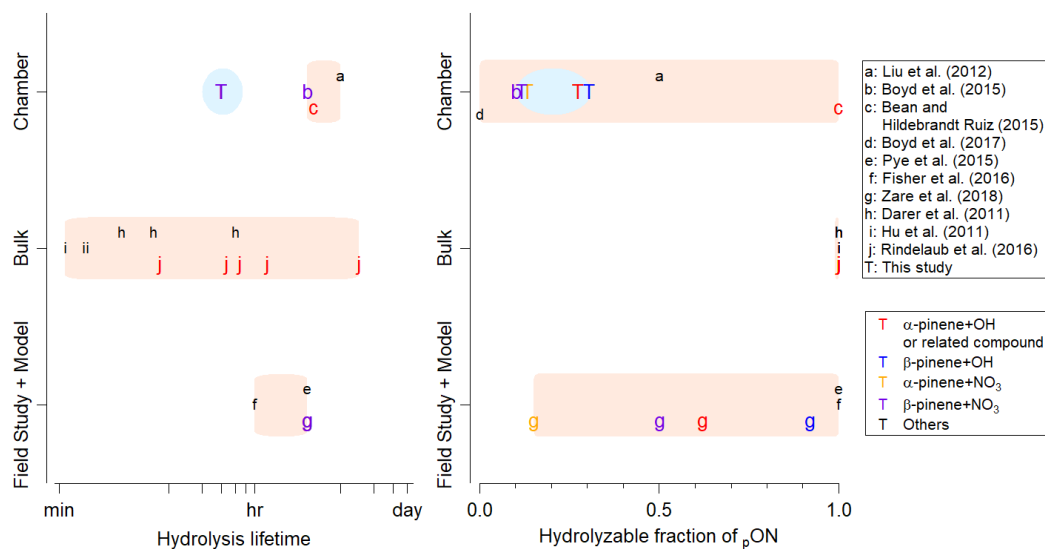
Figure 5. Comparison of hydrolysis lifetime of organic nitrate and hydrolyzable fraction of $_p$ON in

literature. "Chamber" refers to laboratory studies of organic nitrate aerosol via chamber experiments,

"Bulk" refers to laboratory studies of organic nitrate compounds using bulk solution measurements, and

"Model" refers to modeling studies using ambient measurement data as constraints. Data points are colored

by the system of VOC and oxidant condition explored in this study and are alphabetized based on the

reference. Pink shaded regions are ranges reported in literature, while blue shaded regions are ranges

reported in this study.

576
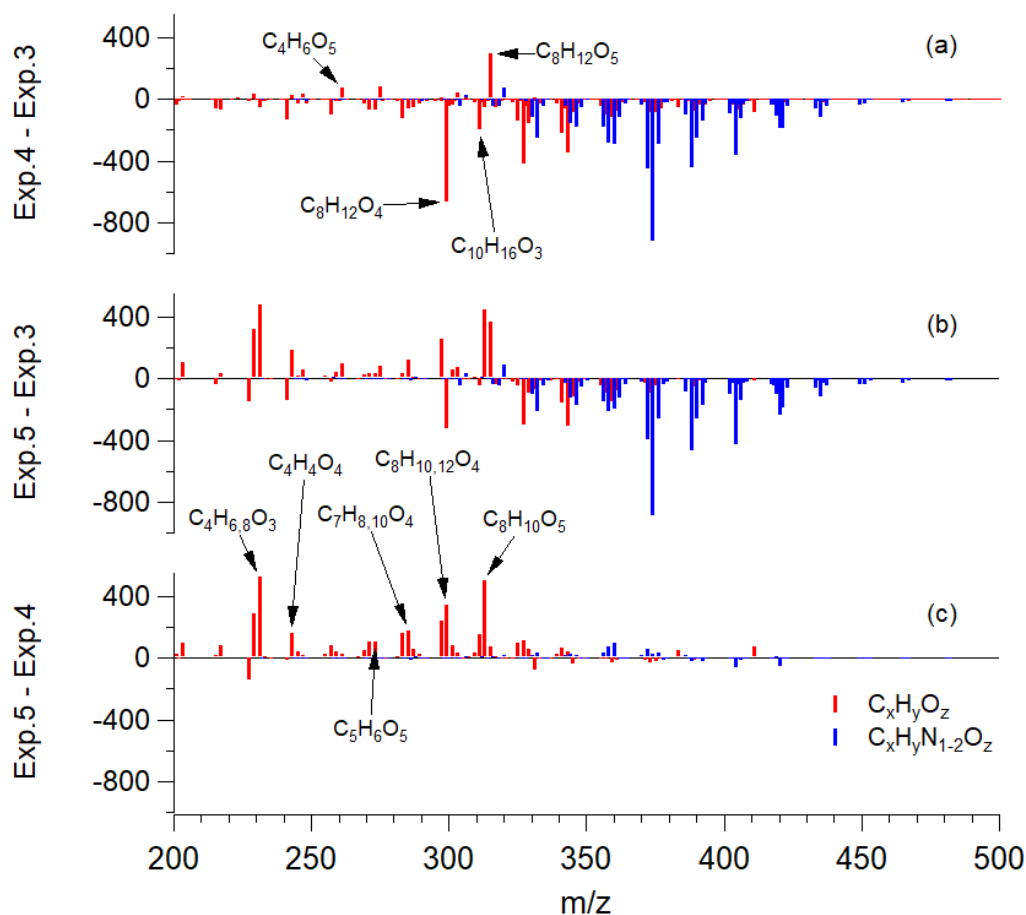
577

578   Figure 6. FIGAERO-HR-ToF-I-CIMS difference mass spectra of SOA in α-pinene+OH. (a) Exp. 4 (high

579   RH, dry AS) minus Exp. 3 (low RH, dry AS). (b) Exp. 5 (high RH, wet AS) minus Exp. 3 (low RH, dry

580   AS). (c) Exp. 5 (high RH, wet AS) minus Exp. 4 (high RH, dry AS). Bars are colored by the difference in

581   chemical composition (i.e., red for $C_xH_yO_z$ and blue for $C_xH_yN_{1-2}O_z$). Prominent masses are labeled with

582   the corresponding chemical formulae without an iodide ion.

583

584   Table 1. Summary of experimental conditions considered in this study.

Exp.	Precursor VOC	Oxidant precursor	Reactor RH	Seed
1	α-pinene (25 ppb)	H_2O_2 (2 ppm), NO (6 ppb min^{-1})	~5 %	Effloresced AS[b]
2	α-pinene (25 ppb)	H_2O_2 (2 ppm), NO (6 ppb min^{-1})	~50-70 %[a]	Deliquesced SA+MS[c]
3	α-pinene (25 ppb)	H_2O_2 (2 ppm), NO (2 ppb min^{-1})	~5 %	Effloresced AS
4	α-pinene (25 ppb)	H_2O_2 (2 ppm), NO (2 ppb min^{-1})	~50-70 %	Effloresced AS
5	α-pinene (25 ppb)	H_2O_2 (2 ppm), NO (2 ppb min^{-1})	~50-70 %	Deliquesced AS
6	β-pinene (25 ppb)	H_2O_2 (2 ppm), NO (6 ppb min^{-1})	~5 %	Effloresced AS
7	β-pinene (25 ppb)	H_2O_2 (2 ppm), NO (6 ppb min^{-1})	~50-70 %	Deliquesced SA+MS
8	α-pinene (12 ppb)	N_2O_5 (80 ppb)	~5 %	Effloresced AS
9	α-pinene (12 ppb)	N_2O_5 (80 ppb)	~60-70 %	Deliquesced SA+MS
10	α-pinene (12 ppb)	N_2O_5 (80 ppb)	~5 %	Effloresced AS
11	α-pinene (12 ppb)	N_2O_5 (80 ppb)	~60-70 %	Deliquesced AS
12	α-pinene (12 ppb)	N_2O_5 (80 ppb), HCHO (25 ppm)	~5 %	Effloresced AS
13	α-pinene (12 ppb)	N_2O_5 (80 ppb), HCHO (25 ppm)	~60-70 %	Deliquesced AS
14	β-pinene (12 ppb)	N_2O_5 (80 ppb)	~5 %	Effloresced AS
15	β-pinene (12 ppb)	N_2O_5 (80 ppb)	~60-70 %	Deliquesced SA+MS

585   [a]The target for the initial reactor RH is ~70 %. However, the irradiation of UV light increases the reactor

586   temperature by several degree Celsius and hence decreases RH.

587   [b]Ammonium sulfate

588   [c]Sulfuric acid and magnesium sulfate

589

590 Table 2. Hydrolysis lifetime and corresponding fraction of hydrolyzable $_pON$.

System	Hydrolysis lifetime	Hydrolyzable fraction $(F_H)^a$
α-pinene+OH	<30 min	23–32 %
β-pinene+OH	<30 min	27–34 %
α-pinene+NO_3	<30 min	9–17 %
β-pinene+NO_3	<30 min	9–15 %

591 [a]Lower or higher limit of hydrolyzable $_pON$ fraction is based on the assumptions that organic moiety of

592 hydrolysis products remains in aerosol or partitions back to the gas phase.

593

References

Aljawhary, D., Lee, A. K. Y., and Abbatt, J. P. D.: High-resolution chemical ionization mass spectrometry (ToF-CIMS): application to study SOA composition and processing, Atmos Meas Tech, 6, 3211-3224, 10.5194/amt-6-3211-2013, 2013.

Aljawhary, D., Zhao, R., Lee, A. K. Y., Wang, C., and Abbatt, J. P. D.: Kinetics, Mechanism, and Secondary Organic Aerosol Yield of Aqueous Phase Photo-oxidation of alpha-Pinene Oxidation Products, J Phys Chem A, 120, 1395-1407, 10.1021/acs.jpca.5b06237, 2016.

Aschmann, S. M., Atkinson, R., and Arey, J.: Products of reaction of OH radicals with alpha-pinene, J Geophys Res-Atmos, 107, Artn 4191

10.1029/2001jd001098, 2002.

Bean, J. K., and Hildebrandt Ruiz, L.: Gas-particle partitioning and hydrolysis of organic nitrates formed from the oxidation of alpha-pinene in environmental chamber experiments, Atmos Chem Phys, 16, 2175-2184, 10.5194/acp-16-2175-2016, 2016.

Berndt, T., and Boge, O.: Products and mechanism of the gas-phase reaction of NO3 radicals with alpha-pinene, J Chem Soc Faraday T, 93, 3021-3027, DOI 10.1039/a702364b, 1997.

Berndt, T., Richters, S., Jokinen, T., Hyttinen, N., Kurten, T., Otkjaer, R. V., Kjaergaard, H. G., Stratmann, F., Herrmann, H., Sipila, M., Kulmala, M., and Ehn, M.: Hydroxyl radical-induced formation of highly oxidized organic compounds, Nat Commun, 7, ARTN 13677

10.1038/ncomms13677, 2016.

Bertram, T. H., Kimmel, J. R., Crisp, T. A., Ryder, O. S., Yatavelli, R. L. N., Thornton, J. A., Cubison, M. J., Gonin, M., and Worsnop, D. R.: A field-deployable, chemical ionization time-of-flight mass spectrometer, Atmos Meas Tech, 4, 1471-1479, 10.5194/amt-4-1471-2011, 2011.

Boschan, R., Merrow, R. T., and Vandolah, R. W.: The Chemistry of Nitrate Esters, Chem Rev, 55, 485-510, DOI 10.1021/cr50003a001, 1955.

Boyd, C. M., Sanchez, J., Xu, L., Eugene, A. J., Nah, T., Tuet, W. Y., Guzman, M. I., and Ng, N. L.: Secondary organic aerosol formation from the beta-pinene+NO3 system: effect of humidity and peroxy radical fate, Atmos Chem Phys, 15, 7497-7522, 10.5194/acp-15-7497-2015, 2015.

Boyd, C. M., Nah, T., Xu, L., Berkemeier, T., and Ng, N. L.: Secondary Organic Aerosol (SOA) from Nitrate Radical Oxidation of Monoterpenes: Effects of Temperature, Dilution, and Humidity on Aerosol Formation, Mixing, and Evaporation, Environ Sci Technol, 51, 7831-7841, 10.1021/acs.est.7b01460, 2017.

Browne, E. C., Min, K. E., Wooldridge, P. J., Apel, E., Blake, D. R., Brune, W. H., Cantrell, C. A., Cubison, M. J., Diskin, G. S., Jimenez, J. L., Weinheimer, A. J., Wennberg, P. O., Wisthaler, A., and Cohen, R. C.: Observations of total RONO2 over the boreal forest: NOx sinks and HNO3 sources, Atmos Chem Phys, 13, 4543-4562, 10.5194/acp-13-4543-2013, 2013.

Bruns, E. A., Perraud, V., Zelenyuk, A., Ezell, M. J., Johnson, S. N., Yu, Y., Imre, D., Finlayson-Pitts, B. J., and Alexander, M. L.: Comparison of FTIR and Particle Mass Spectrometry for the Measurement of Particulate Organic Nitrates, Environ Sci Technol, 44, 1056-1061, 10.1021/es9029864, 2010.

631   Canagaratna, M. R., Jimenez, J. L., Kroll, J. H., Chen, Q., Kessler, S. H., Massoli, P., Hildebrandt Ruiz, L.,
632   Fortner, E., Williams, L. R., Wilson, K. R., Surratt, J. D., Donahue, N. M., Jayne, J. T., and Worsnop, D.
633   R.: Elemental ratio measurements of organic compounds using aerosol mass spectrometry: characterization,
634   improved calibration, and implications, Atmos Chem Phys, 15, 253-272, 10.5194/acp-15-253-2015, 2015.

635   Carlton, A. G., Pinder, R. W., Bhave, P. V., and Pouliot, G. A.: To What Extent Can Biogenic SOA be
636   Controlled?, Environ Sci Technol, 44, 3376-3380, 10.1021/es903506b, 2010.

637   Cerully, K. M., Bougiatioti, A., Hite, J. R., Guo, H., Xu, L., Ng, N. L., Weber, R., and Nenes, A.: On the
638   link between hygroscopicity, volatility, and oxidation state of ambient and water-soluble aerosols in the
639   southeastern United States, Atmos Chem Phys, 15, 8679-8694, 10.5194/acp-15-8679-2015, 2015.

640   Claflin, M. S., and Ziemann, P. J.: Identification and Quantitation of Aerosol Products of the Reaction of
641   beta-Pinene with NO3 Radicals and Implications for Gas- and Particle-Phase Reaction Mechanisms, J Phys
642   Chem A, 122, 3640-3652, 10.1021/acs.jpca.8b00692, 2018.

643   Crounse, J. D., Nielsen, L. B., Jorgensen, S., Kjaergaard, H. G., and Wennberg, P. O.: Autoxidation of
644   Organic Compounds in the Atmosphere, J Phys Chem Lett, 4, 3513-3520, 10.1021/jz4019207, 2013.

645   Darer, A. I., Cole-Filipiak, N. C., O'Connor, A. E., and Elrod, M. J.: Formation and Stability of
646   Atmospherically Relevant Isoprene-Derived Organosulfates and Organonitrates, Environ Sci Technol, 45,
647   1895-1902, 10.1021/es103797z, 2011.

648   Day, D. A., Liu, S., Russell, L. M., and Ziemann, P. J.: Organonitrate group concentrations in submicron
649   particles with high nitrate and organic fractions in coastal southern California, Atmos Environ, 44, 1970-
650   1979, 10.1016/j.atmosenv.2010.02.045, 2010.

651   DeCarlo, P. F., Kimmel, J. R., Trimborn, A., Northway, M. J., Jayne, J. T., Aiken, A. C., Gonin, M., Fuhrer,
652   K., Horvath, T., Docherty, K. S., Worsnop, D. R., and Jimenez, J. L.: Field-deployable, high-resolution,
653   time-of-flight aerosol mass spectrometer, Anal Chem, 78, 8281-8289, 10.1021/ac061249n, 2006.

654   Eddingsaas, N. C., Loza, C. L., Yee, L. D., Chan, M., Schilling, K. A., Chhabra, P. S., Seinfeld, J. H., and
655   Wennberg, P. O.: alpha-pinene photooxidation under controlled chemical conditions - Part 2: SOA yield
656   and composition in low- and high-NOx environments, Atmos Chem Phys, 12, 7413-7427, 10.5194/acp-12-
657   7413-2012, 2012.

658   Ehn, M., Thornton, J. A., Kleist, E., Sipila, M., Junninen, H., Pullinen, I., Springer, M., Rubach, F.,
659   Tillmann, R., Lee, B., Lopez-Hilfiker, F., Andres, S., Acir, I. H., Rissanen, M., Jokinen, T., Schobesberger,
660   S., Kangasluoma, J., Kontkanen, J., Nieminen, T., Kurten, T., Nielsen, L. B., Jorgensen, S., Kjaergaard, H.
661   G., Canagaratna, M., Dal Maso, M., Berndt, T., Petaja, T., Wahner, A., Kerminen, V. M., Kulmala, M.,
662   Worsnop, D. R., Wildt, J., and Mentel, T. F.: A large source of low-volatility secondary organic aerosol,
663   Nature, 506, 476-+, 10.1038/nature13032, 2014.

664   Ervens, B., Turpin, B. J., and Weber, R. J.: Secondary organic aerosol formation in cloud droplets and
665   aqueous particles (aqSOA): a review of laboratory, field and model studies, Atmos Chem Phys, 11, 11069-
666   11102, 10.5194/acp-11-11069-2011, 2011.

667   Farmer, D. K., Matsunaga, A., Docherty, K. S., Surratt, J. D., Seinfeld, J. H., Ziemann, P. J., and Jimenez,
668   J. L.: Response of an aerosol mass spectrometer to organonitrates and organosulfates and implications for
669   atmospheric chemistry, P Natl Acad Sci USA, 107, 6670-6675, 10.1073/pnas.0912340107, 2010.

Faxon, C., Hammes, J., Le Breton, M., Pathak, R. K., and Hallquist, M.: Characterization of organic nitrate constituents of secondary organic aerosol (SOA) from nitrate-radical-initiated oxidation of limonene using high-resolution chemical ionization mass spectrometry, Atmos Chem Phys, 18, 5467-5481, 10.5194/acp-18-5467-2018, 2018.

Fisher, J. A., Jacob, D. J., Travis, K. R., Kim, P. S., Marais, E. A., Miller, C. C., Yu, K. R., Zhu, L., Yantosca, R. M., Sulprizio, M. P., Mao, J. Q., Wennberg, P. O., Crounse, J. D., Teng, A. P., Nguyen, T. B., St Clair, J. M., Cohen, R. C., Romer, P., Nault, B. A., Wooldridge, P. J., Jimenez, J. L., Campuzano-Jost, P., Day, D. A., Hu, W. W., Shepson, P. B., Xiong, F. L. Z., Blake, D. R., Goldstein, A. H., Misztal, P. K., Hanisco, T. F., Wolfe, G. M., Ryerson, T. B., Wisthaler, A., and Mikoviny, T.: Organic nitrate chemistry and its implications for nitrogen budgets in an isoprene- and monoterpene-rich atmosphere: constraints from aircraft (SEAC(4)RS) and ground-based (SOAS) observations in the Southeast US, Atmos Chem Phys, 16, 5969-5991, 10.5194/acp-16-5969-2016, 2016.

Fry, J. L., Kiendler-Scharr, A., Rollins, A. W., Wooldridge, P. J., Brown, S. S., Fuchs, H., Dube, W., Mensah, A., dal Maso, M., Tillmann, R., Dorn, H. P., Brauers, T., and Cohen, R. C.: Organic nitrate and secondary organic aerosol yield from NO3 oxidation of beta-pinene evaluated using a gas-phase kinetics/aerosol partitioning model, Atmos Chem Phys, 9, 1431-1449, DOI 10.5194/acp-9-1431-2009, 2009.

Fry, J. L., Draper, D. C., Zarzana, K. J., Campuzano-Jost, P., Day, D. A., Jimenez, J. L., Brown, S. S., Cohen, R. C., Kaser, L., Hansel, A., Cappellin, L., Karl, T., Roux, A. H., Turnipseed, A., Cantrell, C., Lefer, B. L., and Grossberg, N.: Observations of gas- and aerosol-phase organic nitrates at BEACHON-RoMBAS 2011, Atmos Chem Phys, 13, 8585-8605, 10.5194/acp-13-8585-2013, 2013.

Fry, J. L., Draper, D. C., Barsanti, K. C., Smith, J. N., Ortega, J., Winkle, P. M., Lawler, M. J., Brown, S. S., Edwards, P. M., Cohen, R. C., and Lee, L.: Secondary Organic Aerosol Formation and Organic Nitrate Yield from NO3 Oxidation of Biogenic Hydrocarbons, Environ Sci Technol, 48, 11944-11953, 10.1021/es502204x, 2014.

Fry, J. L., Brown, S. S., Middlebrook, A. M., Edwards, P. M., Campuzano-Jost, P., Day, D. A., Jimenez, J. L., Allen, H. M., Ryerson, T. B., Pollack, I., Graus, M., Warneke, C., de Gouw, J. A., Brock, C. A., Gilman, J., Lerner, B. M., Dube, W. P., Liao, J., and Welti, A.: Secondary organic aerosol (SOA) yields from NO3 radical + isoprene based on nighttime aircraft power plant plume transects, Atmos Chem Phys, 18, 11663-11682, 10.5194/acp-18-11663-2018, 2018.

Goldstein, A. H., and Galbally, I. E.: Known and unexplored organic constituents in the earth's atmosphere, Environ Sci Technol, 41, 1514-1521, DOI 10.1021/es072476p, 2007.

Griffin, R. J., Cocker, D. R., Flagan, R. C., and Seinfeld, J. H.: Organic aerosol formation from the oxidation of biogenic hydrocarbons, J Geophys Res-Atmos, 104, 3555-3567, Doi 10.1029/1998jd100049, 1999.

Guenther, A. B., Jiang, X., Heald, C. L., Sakulyanontvittaya, T., Duhl, T., Emmons, L. K., and Wang, X.: The Model of Emissions of Gases and Aerosols from Nature version 2.1 (MEGAN2.1): an extended and updated framework for modeling biogenic emissions, Geosci Model Dev, 5, 1471-1492, 10.5194/gmd-5-1471-2012, 2012.

Hallquist, M., Wangberg, I., Ljungstrom, E., Barnes, I., and Becker, K. H.: Aerosol and product yields from NO3 radical-initiated oxidation of selected monoterpenes, Environ Sci Technol, 33, 553-559, DOI 10.1021/es980292s, 1999.

711   Hoyle, C. R., Boy, M., Donahue, N. M., Fry, J. L., Glasius, M., Guenther, A., Hallar, A. G., Hartz, K. H.,
712   Petters, M. D., Petaja, T., Rosenoern, T., and Sullivan, A. P.: A review of the anthropogenic influence on
713   biogenic secondary organic aerosol, Atmos Chem Phys, 11, 321-343, 10.5194/acp-11-321-2011, 2011.

714   Hu, K. S., Darer, A. I., and Elrod, M. J.: Thermodynamics and kinetics of the hydrolysis of atmospherically
715   relevant organonitrates and organosulfates, Atmos Chem Phys, 11, 8307-8320, 10.5194/acp-11-8307-2011,
716   2011.

717   Huang, W., Saathoff, H., Shen, X. L., Ramisetty, R., Leisner, T., and Mohr, C.: Chemical Characterization
718   of Highly Functionalized Organonitrates Contributing to Night-Time Organic Aerosol Mass Loadings and
719   Particle Growth, Environ Sci Technol, 53, 1165-1174, 10.1021/acs.est.8b05826, 2019.

720   Huang, Y. L., Zhao, R., Charan, S. M., Kenseth, C. M., Zhang, X., and Seinfeld, J. H.: Unified Theory of
721   Vapor-Wall Mass Transport in Teflon-Walled Environmental Chambers, Environ Sci Technol, 52, 2134-
722   2142, 10.1021/acs.est.7b05575, 2018.

723   Jacobs, M. I., Burke, W. J., and Elrod, M. J.: Kinetics of the reactions of isoprene-derived hydroxynitrates:
724   gas phase epoxide formation and solution phase hydrolysis, Atmos Chem Phys, 14, 8933-8946,
725   10.5194/acp-14-8933-2014, 2014.

726   Jenkin, M. E., Saunders, S. M., and Pilling, M. J.: The tropospheric degradation of volatile organic
727   compounds: A protocol for mechanism development, Atmos Environ, 31, 81-104, Doi 10.1016/S1352-
728   2310(96)00105-7, 1997.

729   Jokinen, T., Berndt, T., Makkonen, R., Kerminen, V. M., Junninen, H., Paasonen, P., Stratmann, F.,
730   Herrmann, H., Guenther, A. B., Worsnop, D. R., Kulmala, M., Ehn, M., and Sipila, M.: Production of
731   extremely low volatile organic compounds from biogenic emissions: Measured yields and atmospheric
732   implications, P Natl Acad Sci USA, 112, 7123-7128, 10.1073/pnas.1423977112, 2015.

733   Kanakidou, M., Seinfeld, J. H., Pandis, S. N., Barnes, I., Dentener, F. J., Facchini, M. C., Van Dingenen,
734   R., Ervens, B., Nenes, A., Nielsen, C. J., Swietlicki, E., Putaud, J. P., Balkanski, Y., Fuzzi, S., Horth, J.,
735   Moortgat, G. K., Winterhalter, R., Myhre, C. E. L., Tsigaridis, K., Vignati, E., Stephanou, E. G., and
736   Wilson, J.: Organic aerosol and global climate modelling: a review, Atmos Chem Phys, 5, 1053-1123, DOI
737   10.5194/acp-5-1053-2005, 2005.

738   Kebabian, P. L., Herndon, S. C., and Freedman, A.: Detection of nitrogen dioxide by cavity attenuated
739   phase shift spectroscopy, Anal Chem, 77, 724-728, 10.1021/ac048715y, 2005.

740   Kiendler-Scharr, A., Mensah, A. A., Friese, E., Topping, D., Nemitz, E., Prevot, A. S. H., Aijala, M., Allan,
741   J., Canonaco, F., Canagaratna, M., Carbone, S., Crippa, M., Dall Osto, M., Day, D. A., De Carlo, P., Di
742   Marco, C. F., Elbern, H., Eriksson, A., Freney, E., Hao, L., Herrmann, H., Hildebrandt, L., Hillamo, R.,
743   Jimenez, J. L., Laaksonen, A., McFiggans, G., Mohr, C., O'Dowd, C., Otjes, R., Ovadnevaite, J., Pandis, S.
744   N., Poulain, L., Schlag, P., Sellegri, K., Swietlicki, E., Tiitta, P., Vermeulen, A., Wahner, A., Worsnop, D.,
745   and Wu, H. C.: Ubiquity of organic nitrates from nighttime chemistry in the European submicron aerosol,
746   Geophys Res Lett, 43, 7735-7744, 10.1002/2016gl069239, 2016.

747   Krechmer, J. E., Pagonis, D., Ziemann, P. J., and Jimenez, J. L.: Quantification of Gas-Wall Partitioning in
748   Teflon Environmental Chambers Using Rapid Bursts of Low-Volatility Oxidized Species Generated in
749   Situ, Environ Sci Technol, 50, 5757-5765, 10.1021/acs.est.6b00606, 2016.

750 Kroll, J. H., and Seinfeld, J. H.: Chemistry of secondary organic aerosol: Formation and evolution of low-
751 volatility organics in the atmosphere, Atmos Environ, 42, 3593-3624, 10.1016/j.atmosenv.2008.01.003,
752 2008.

753 La, Y. S., Camredon, M., Ziemann, P. J., Valorso, R., Matsunaga, A., Lannuque, V., Lee-Taylor, J., Hodzic,
754 A., Madronich, S., and Aumont, B.: Impact of chamber wall loss of gaseous organic compounds on
755 secondary organic aerosol formation: explicit modeling of SOA formation from alkane and alkene
756 oxidation, Atmos Chem Phys, 16, 1417-1431, 10.5194/acp-16-1417-2016, 2016.

757 Lee, B. H., Lopez-Hilfiker, F. D., Mohr, C., Kurten, T., Worsnop, D. R., and Thornton, J. A.: An Iodide-
758 Adduct High-Resolution Time-of-Flight Chemical-Ionization Mass Spectrometer: Application to
759 Atmospheric Inorganic and Organic Compounds, Environ Sci Technol, 48, 6309-6317, 10.1021/es500362a,
760 2014.

761 Lee, B. H., Mohr, C., Lopez-Hilfiker, F. D., Lutz, A., Hallquist, M., Lee, L., Romer, P., Cohen, R. C., Iyer,
762 S., Kurten, T., Hu, W. W., Day, D. A., Campuzano-Jost, P., Jimenez, J. L., Xu, L., Ng, N. L., Guo, H. Y.,
763 Weber, R. J., Wild, R. J., Brown, S. S., Koss, A., de Gouw, J., Olson, K., Goldstein, A. H., Seco, R., Kim,
764 S., McAvey, K., Shepson, P. B., Starn, T., Baumann, K., Edgerton, E. S., Liu, J. M., Shilling, J. E., Miller,
765 D. O., Brune, W., Schobesberger, S., D'Ambro, E. L., and Thornton, J. A.: Highly functionalized organic
766 nitrates in the southeast United States: Contribution to secondary organic aerosol and reactive nitrogen
767 budgets, P Natl Acad Sci USA, 113, 1516-1521, 10.1073/pnas.1508108113, 2016.

768 Liu, S., Ahlm, L., Day, D. A., Russell, L. M., Zhao, Y. L., Gentner, D. R., Weber, R. J., Goldstein, A. H.,
769 Jaoui, M., Offenberg, J. H., Kleindienst, T. E., Rubitschun, C., Surratt, J. D., Sheesley, R. J., and Scheller,
770 S.: Secondary organic aerosol formation from fossil fuel sources contribute majority of summertime organic
771 mass at Bakersfield, J Geophys Res-Atmos, 117, Artn D00v26

772 10.1029/2012jd018170, 2012a.

773 Liu, S., Shilling, J. E., Song, C., Hiranuma, N., Zaveri, R. A., and Russell, L. M.: Hydrolysis of
774 Organonitrate Functional Groups in Aerosol Particles, Aerosol Sci Tech, 46, 1359-1369,
775 10.1080/02786826.2012.716175, 2012b.

776 Lopez-Hilfiker, F. D., Mohr, C., Ehn, M., Rubach, F., Kleist, E., Wildt, J., Mentel, T. F., Lutz, A., Hallquist,
777 M., Worsnop, D., and Thornton, J. A.: A novel method for online analysis of gas and particle composition:
778 description and evaluation of a Filter Inlet for Gases and AEROsols (FIGAERO), Atmos Meas Tech, 7,
779 983-1001, 10.5194/amt-7-983-2014, 2014.

780 Loza, C. L., Chan, A. W. H., Galloway, M. M., Keutsch, F. N., Flagan, R. C., and Seinfeld, J. H.:
781 Characterization of Vapor Wall Loss in Laboratory Chambers, Environ Sci Technol, 44, 5074-5078,
782 10.1021/es100727v, 2010.

783 Matsunaga, A., and Ziemann, P. J.: Gas-Wall Partitioning of Organic Compounds in a Teflon Film Chamber
784 and Potential Effects on Reaction Product and Aerosol Yield Measurements, Aerosol Sci Tech, 44, 881-
785 892, 10.1080/02786826.2010.501044, 2010.

786 Mcvay, R. C., Cappa, C. D., and Seinfeld, J. H.: Vapor-Wall Deposition in Chambers: Theoretical
787 Considerations, Environ Sci Technol, 48, 10251-10258, 10.1021/es502170j, 2014.

788 Muller, J. F., Peeters, J., and Stavrakou, T.: Fast photolysis of carbonyl nitrates from isoprene, Atmos Chem
789 Phys, 14, 2497-2508, 10.5194/acp-14-2497-2014, 2014.

790 Nah, T., Sanchez, J., Boyd, C. M., and Ng, N. L.: Photochemical Aging of alpha-pinene and beta-pinene
791 Secondary Organic Aerosol formed from Nitrate Radical Oxidation, Environ Sci Technol, 50, 222-231,
792 10.1021/acs.est.5b04594, 2016.

793 Ng, N. L., Herndon, S. C., Trimborn, A., Canagaratna, M. R., Croteau, P. L., Onasch, T. B., Sueper, D.,
794 Worsnop, D. R., Zhang, Q., Sun, Y. L., and Jayne, J. T.: An Aerosol Chemical Speciation Monitor (ACSM)
795 for Routine Monitoring of the Composition and Mass Concentrations of Ambient Aerosol, Aerosol Sci
796 Tech, 45, 780-794, Pii 934555189

797 10.1080/02786826.2011.560211, 2011.

798 Ng, N. L., Brown, S. S., Archibald, A. T., Atlas, E., Cohen, R. C., Crowley, J. N., Day, D. A., Donahue, N.
799 M., Fry, J. L., Fuchs, H., Griffin, R. J., Guzman, M. I., Herrmann, H., Hodzic, A., Iinuma, Y., Jimenez, J.
800 L., Kiendler-Scharr, A., Lee, B. H., Luecken, D. J., Mao, J. Q., McLaren, R., Mutzel, A., Osthoff, H. D.,
801 Ouyang, B., Picquet-Varrault, B., Platt, U., Pye, H. O. T., Rudich, Y., Schwantes, R. H., Shiraiwa, M.,
802 Stutz, J., Thornton, J. A., Tilgner, A., Williams, B. J., and Zaveri, R. A.: Nitrate radicals and biogenic
803 volatile organic compounds: oxidation, mechanisms, and organic aerosol, Atmos Chem Phys, 17, 2103-
804 2162, 10.5194/acp-17-2103-2017, 2017.

805 Nguyen, T. B., Crounse, J. D., Teng, A. P., Clair, J. M. S., Paulot, F., Wolfe, G. M., and Wennberg, P. O.:
806 Rapid deposition of oxidized biogenic compounds to a temperate forest, P Natl Acad Sci USA, 112, E392-
807 E401, 10.1073/pnas.1418702112, 2015.

808 Noziere, B., Barnes, I., and Becker, K. H.: Product study and mechanisms of the reactions of alpha-pinene
809 and of pinonaldehyde with OH radicals, J Geophys Res-Atmos, 104, 23645-23656, Doi
810 10.1029/1999jd900778, 1999.

811 Pankow, J. F.: An Absorption-Model of Gas-Particle Partitioning of Organic-Compounds in the
812 Atmosphere, Atmos Environ, 28, 185-188, Doi 10.1016/1352-2310(94)90093-0, 1994.

813 Pankow, J. F., and Asher, W. E.: SIMPOL.1: a simple group contribution method for predicting vapor
814 pressures and enthalpies of vaporization of multifunctional organic compounds, Atmos Chem Phys, 8,
815 2773-2796, DOI 10.5194/acp-8-2773-2008, 2008.

816 Perring, A. E., Pusede, S. E., and Cohen, R. C.: An Observational Perspective on the Atmospheric Impacts
817 of Alkyl and Multifunctional Nitrates on Ozone and Secondary Organic Aerosol, Chem Rev, 113, 5848-
818 5870, 10.1021/cr300520x, 2013.

819 Petters, M. D., and Kreidenweis, S. M.: A single parameter representation of hygroscopic growth and cloud
820 condensation nucleus activity, Atmos Chem Phys, 7, 1961-1971, DOI 10.5194/acp-7-1961-2007, 2007.

821 Pye, H. O. T., Luecken, D. J., Xu, L., Boyd, C. M., Ng, N. L., Baker, K. R., Ayres, B. R., Bash, J. O.,
822 Baumann, K., Carter, W. P. L., Edgerton, E., Fry, J. L., Hutzell, W. T., Schwede, D. B., and Shepson, P.
823 B.: Modeling the Current and Future Roles of Particulate Organic Nitrates in the Southeastern United States,
824 Environ Sci Technol, 49, 14195-14203, 10.1021/acs.est.5b03738, 2015.

825 Pye, H. O. T., D'Ambro, E. L., Lee, B., Schobesberger, S., Takeuchi, M., Zhao, Y., Lopez-Hilfiker, F., Liu,
826 J. M., Shilling, J. E., Xing, J., Mathur, R., Middlebrook, A. M., Liao, J., Welti, A., Graus, M., Warneke, C.,
827 de Gouw, J. A., Holloway, J. S., Ryerson, T. B., Pollack, I. B., and Thornton, J. A.: Anthropogenic
828 enhancements to production of highly oxygenated molecules from autoxidation, P Natl Acad Sci USA, 116,
829 6641-6646, 10.1073/pnas.1810774116, 2019.

830 Rindelaub, J. D., McAvey, K. M., and Shepson, P. B.: The photochemical production of organic nitrates
831 from alpha-pinene and loss via acid-dependent particle phase hydrolysis, Atmos Environ, 100, 193-201,
832 2015.

833 Rindelaub, J. D., Borca, C. H., Hostetler, M. A., Slade, J. H., Lipton, M. A., Slipchenko, L. V., and Shepson,
834 P. B.: The acid-catalyzed hydrolysis of an alpha-pinene-derived organic nitrate: kinetics, products, reaction
835 mechanisms, and atmospheric impact, Atmos Chem Phys, 16, 15425-15432, 10.5194/acp-16-15425-2016,
836 2016.

837 Rollins, A. W., Browne, E. C., Min, K. E., Pusede, S. E., Wooldridge, P. J., Gentner, D. R., Goldstein, A.
838 H., Liu, S., Day, D. A., Russell, L. M., and Cohen, R. C.: Evidence for NOx Control over Nighttime SOA
839 Formation, Science, 337, 1210-1212, 10.1126/science.1221520, 2012.

840 Rollins, A. W., Pusede, S., Wooldridge, P., Min, K. E., Gentner, D. R., Goldstein, A. H., Liu, S., Day, D.
841 A., Russell, L. M., Rubitschun, C. L., Surratt, J. D., and Cohen, R. C.: Gas/particle partitioning of total
842 alkyl nitrates observed with TD-LIF in Bakersfield, J Geophys Res-Atmos, 118, 6651-6662,
843 10.1002/jgrd.50522, 2013.

844 Romonosky, D. E., Li, Y., Shiraiwa, M., Laskin, A., Laskin, J., and Nizkorodov, S. A.: Aqueous
845 Photochemistry of Secondary Organic Aerosol of alpha-Pinene and alpha-Humulene Oxidized with Ozone,
846 Hydroxyl Radical, and Nitrate Radical, J Phys Chem A, 121, 1298-1309, 10.1021/acs.jpca.6b10900, 2017.

847 Ruggeri, G., Bernhard, F. A., Henderson, B. H., and Takahama, S.: Model-measurement comparison of
848 functional group abundance in alpha-pinene and 1,3,5-trimethylbenzene secondary organic aerosol
849 formation, Atmos Chem Phys, 16, 8729-8747, 10.5194/acp-16-8729-2016, 2016.

850 Russell, L. M., Bahadur, R., and Ziemann, P. J.: Identifying organic aerosol sources by comparing
851 functional group composition in chamber and atmospheric particles, P Natl Acad Sci USA, 108, 3516-3521,
852 10.1073/pnas.1006461108, 2011.

853 Sanchez, J., Tanner, D. J., Chen, D. X., Huey, L. G., and Ng, N. L.: A new technique for the direct detection
854 of HO2 radicals using bromide chemical ionization mass spectrometry (Br-CIMS): initial characterization,
855 Atmos Meas Tech, 9, 3851-3861, 10.5194/amt-9-3851-2016, 2016.

856 Saunders, S. M., Jenkin, M. E., Derwent, R. G., and Pilling, M. J.: Protocol for the development of the
857 Master Chemical Mechanism, MCM v3 (Part A): tropospheric degradation of non-aromatic volatile organic
858 compounds, Atmos Chem Phys, 3, 161-180, DOI 10.5194/acp-3-161-2003, 2003.

859 Schwantes, R. H., Teng, A. P., Nguyen, T. B., Coggon, M. M., Crounse, J. D., St Clair, J. M., Zhang, X.,
860 Schilling, K. A., Seinfeld, J. H., and Wennberg, P. O.: Isoprene NO3 Oxidation Products from the RO2 +
861 HO2 Pathway, J Phys Chem A, 119, 10158-10171, 10.1021/acs.jpca.5b06355, 2015.

862 Seinfeld, J. H., and Pandis, S. N.: Atmospheric chemistry and physics : from air pollution to climate change,
863 2016.

864 Shilling, J. E., Zaveri, R. A., Fast, J. D., Kleinman, L., Alexander, M. L., Canagaratna, M. R., Fortner, E.,
865 Hubbe, J. M., Jayne, J. T., Sedlacek, A., Setyan, A., Springston, S., Worsnop, D. R., and Zhang, Q.:
866 Enhanced SOA formation from mixed anthropogenic and biogenic emissions during the CARES campaign,
867 Atmos Chem Phys, 13, 2091-2113, 10.5194/acp-13-2091-2013, 2013.

Shrivastava, M., Andreae, M. O., Artaxo, P., Barbosa, H. M. J., Berg, L. K., Brito, J., Ching, J., Easter, R. C., Fan, J. W., Fast, J. D., Feng, Z., Fuentes, J. D., Glasius, M., Goldstein, A. H., Alves, E. G., Gomes, H., Gu, D., Guenther, A., Jathar, S. H., Kim, S., Liu, Y., Lou, S. J., Martin, S. T., McNeill, V. F., Medeiros, A., de Sa, S. S., Shilling, J. E., Springston, S. R., Souza, R. A. F., Thornton, J. A., Isaacman-VanWertz, G., Yee, L. D., Ynoue, R., Zaveri, R. A., Zelenyuk, A., and Zhao, C.: Urban pollution greatly enhances formation of natural aerosols over the Amazon rainforest, Nat Commun, 10, ARTN 1046

10.1038/s41467-019-08909-4, 2019.

Slade, J. H., de Perre, C., Lee, L., and Shepson, P. B.: Nitrate radical oxidation of gamma-terpinene: hydroxy nitrate, total organic nitrate, and secondary organic aerosol yields, Atmos Chem Phys, 17, 8635-8650, 10.5194/acp-17-8635-2017, 2017.

Song, M., Marcolli, C., Krieger, U. K., Zuend, A., and Peter, T.: Liquid-liquid phase separation in aerosol particles: Dependence on O:C, organic functionalities, and compositional complexity, Geophys Res Lett, 39, 10.1029/2012gl052807, 2012.

Spittler, M., Barnes, I., Bejan, I., Brockmann, K. J., Benter, T., and Wirtz, K.: Reactions of NO3 radicals with limonene and alpha-pinene: Product and SOA formation, Atmos Environ, 40, S116-S127, 10.1016/j.atmosenv.2005.09.093, 2006.

Spracklen, D. V., Jimenez, J. L., Carslaw, K. S., Worsnop, D. R., Evans, M. J., Mann, G. W., Zhang, Q., Canagaratna, M. R., Allan, J., Coe, H., McFiggans, G., Rap, A., and Forster, P.: Aerosol mass spectrometer constraint on the global secondary organic aerosol budget, Atmos Chem Phys, 11, 12109-12136, 10.5194/acp-11-12109-2011, 2011.

Stark, H., Yatavelli, R. L. N., Thompson, S. L., Kang, H., Krechmer, J. E., Kimmel, J. R., Palm, B. B., Hu, W. W., Hayes, P. L., Day, D. A., Campuzano-Jost, P., Canagaratna, M. R., Jayne, J. T., Worsnop, D. R., and Jimenez, J. L.: Impact of Thermal Decomposition on Thermal Desorption Instruments: Advantage of Thermogram Analysis for Quantifying Volatility Distributions of Organic Species, Environ Sci Technol, 51, 8491-8500, 10.1021/acs.est.7b00160, 2017.

Takeuchi, M., and Ng, N. L.: Organic Nitrates and Secondary Organic Aerosol (SOA) Formation from Oxidation of Biogenic Volatile Organic Compounds, Acs Sym Ser, 1299, 105-125, 2018.

Wangberg, I., Barnes, I., and Becker, K. H.: Product and mechanistic study of the reaction of NO3 radicals with alpha-pinene, Environ Sci Technol, 31, 2130-2135, DOI 10.1021/es960958n, 1997.

Wayne, R. P., Barnes, I., Biggs, P., Burrows, J. P., Canosamas, C. E., Hjorth, J., Lebras, G., Moortgat, G. K., Perner, D., Poulet, G., Restelli, G., and Sidebottom, H.: The Nitrate Radical - Physics, Chemistry, and the Atmosphere, Atmos Environ a-Gen, 25, 1-203, Doi 10.1016/0960-1686(91)90192-A, 1991.

Weber, R. J., Sullivan, A. P., Peltier, R. E., Russell, A., Yan, B., Zheng, M., de Gouw, J., Warneke, C., Brock, C., Holloway, J. S., Atlas, E. L., and Edgerton, E.: A study of secondary organic aerosol formation in the anthropogenic-influenced southeastern United States, J Geophys Res-Atmos, 112, Artn D13302

10.1029/2007jd008408, 2007.

Xu, L., Guo, H. Y., Boyd, C. M., Klein, M., Bougiatioti, A., Cerully, K. M., Hite, J. R., Isaacman-VanWertz, G., Kreisberg, N. M., Knote, C., Olson, K., Koss, A., Goldstein, A. H., Hering, S. V., de Gouw, J., Baumann, K., Lee, S. H., Nenes, A., Weber, R. J., and Ng, N. L.: Effects of anthropogenic emissions on aerosol

907   formation from isoprene and monoterpenes in the southeastern United States (vol 112, pg 37, 2015), P Natl
908   Acad Sci USA, 112, E4509-E4509, 10.1073/pnas.1512279112, 2015a.

909   Xu, L., Suresh, S., Guo, H., Weber, R. J., and Ng, N. L.: Aerosol characterization over the southeastern
910   United States using high-resolution aerosol mass spectrometry: spatial and seasonal variation of aerosol
911   composition and sources with a focus on organic nitrates, Atmos Chem Phys, 15, 7307-7336, 10.5194/acp-
912   15-7307-2015, 2015b.

913   Xu, L., Pye, H. O. T., He, J., Chen, Y. L., Murphy, B. N., and Ng, N. L.: Experimental and model estimates
914   of the contributions from biogenic monoterpenes and sesquiterpenes to secondary organic aerosol in the
915   southeastern United States, Atmos Chem Phys, 18, 12613-12637, 10.5194/acp-18-12613-2018, 2018a.

916   Xu, L., Moller, K. H., Crounse, J. D., Otkjwr, R. V., Kjaergaard, H. G., and Wennberg, P. O.: Unimolecular
917   Reactions of Peroxy Radicals Formed in the Oxidation of alpha-Pinene and beta-Pinene by Hydroxyl
918   Radicals, J Phys Chem A, 123, 1661-1674, 10.1021/acs.jpca.8b11726, 2019.

919   Xu, W., Lambe, A., Silva, P., Hu, W. W., Onasch, T., Williams, L., Croteau, P., Zhang, X., Renbaum-
920   Wolff, L., Fortner, E., Jimenez, J. L., Jayne, J., Worsnop, D., and Canagaratna, M.: Laboratory evaluation
921   of species-dependent relative ionization efficiencies in the Aerodyne Aerosol Mass Spectrometer, Aerosol
922   Sci Tech, 52, 626-641, 10.1080/02786826.2018.1439570, 2018b.

923   Zare, A., Romer, P. S., Nguyen, T., Keutsch, F. N., Skog, K., and Cohen, R. C.: A comprehensive organic
924   nitrate chemistry: insights into the lifetime of atmospheric organic nitrates, Atmos Chem Phys, 18, 15419-
925   15436, 10.5194/acp-18-15419-2018, 2018.

926   Zhang, H. F., Yee, L. D., Lee, B. H., Curtis, M. P., Worton, D. R., Isaacman-VanWertz, G., Offenberg, J.
927   H., Lewandowski, M., Kleindienst, T. E., Beaver, M. R., Holder, A. L., Lonneman, W. A., Docherty, K. S.,
928   Jaoui, M., Pye, H. O. T., Hu, W. W., Day, D. A., Campuzano-Jost, P., Jimenez, J. L., Guo, H. Y., Weber,
929   R. J., de Gouw, J., Koss, A. R., Edgerton, E. S., Brune, W., Mohr, C., Lopez-Hilfiker, F. D., Lutz, A.,
930   Kreisberg, N. M., Spielman, S. R., Hering, S. V., Wilson, K. R., Thornton, J. A., and Goldstein, A. H.:
931   Monoterpenes are the largest source of summertime organic aerosol in the southeastern United States, P
932   Natl Acad Sci USA, 115, 2038-2043, 10.1073/pnas.1717513115, 2018.

933   Zhang, X., Cappa, C. D., Jathar, S. H., Mcvay, R. C., Ensberg, J. J., Kleeman, M. J., and Seinfeld, J. H.:
934   Influence of vapor wall loss in laboratory chambers on yields of secondary organic aerosol, P Natl Acad
935   Sci USA, 111, 5802-5807, 10.1073/pnas.1404727111, 2014.

936   Zhang, X., Schwantes, R. H., McVay, R. C., Lignell, H., Coggon, M. M., Flagan, R. C., and Seinfeld, J. H.:
937   Vapor wall deposition in Teflon chambers, Atmos Chem Phys, 15, 4197-4214, 10.5194/acp-15-4197-2015,
938   2015.

939   Ziemann, P. J., and Atkinson, R.: Kinetics, products, and mechanisms of secondary organic aerosol
940   formation, Chem Soc Rev, 41, 6582-6605, 10.1039/c2cs35122f, 2012.

941